Equalization for OFDM over Doubly-Selective Channels*

Imad Barhumi[1†], Geert Leus[2‡], and Marc Moonen[1]

[1]K.U.Leuven-ESAT/SCD-SISTA, Kasteelpark Arenberg 10, B-3001 Heverlee, Belgium

[2] T.U.Delft-EE Department, Mekelweg 4, 2628CD Delft, The Netherlands

E-mail: {imad.barhumi,marc.moonen}@esat.kuleuven.ac.be, leus@cas.et.tudelft.nl

Submitted to: IEEE Transactions on Signal Processing

Date : July 6, 2004

Ass. Editor: A. Swami

Manuscript no.: T-SP-02499-2004

Revised: October 13, 2004

* This research work was carried out at the ESAT laboratory of the Katholieke Universiteit Leuven, in the frame of Belgian Programme on Interuniversity Attraction Poles, initiated by the Belgian Federal Science Policy Office IUAP P5/22 ('Dynamical Systems and Control: Computation, Identification and Modelling') and P5/11 ('Mobile multimedia communication systems and networks'), the Concerted Research Action GOA-MEFISTO-666 (Mathematical Engineering for Information and Communication Systems Technology) of the Flemish Government, and Research Project FWO nr.G.0196.02 ('Design of efficient communication techniques for wireless time-dispersive multi-user MIMO systems'). The scientific responsibility is assumed by its authors.

† Partly supported by the Palestinian European Academic Cooperation in Education (PEACE) Programme.

‡ Supported by NWO-STW under the VICI program (DTC.5893).

CONTENTS

I Introduction 3

II System Model 5

III Basis Expansion Channel Model 7

IV Time-Domain Equalization 7

V Frequency-Domain Per-Tone Equalization 12

VI Efficient Implementation of the PTEQ 14

VII Simulations 17

VIII Conclusions 19

References 20

LIST OF FIGURES

1 System Model. 22

2 BEM channel equivalent. 22

3 TEQ equivalent figure. 22

4 Sliding FFT of the q'th modulated version of the received sequence $y^{(r)}[n]$. 23

5 Low complexity PTEQ. 23

6 BER vs. SNR for TEQ and PTEQ, $N_r = 1$ receive antenna. 24

7 BER vs. SNR for TEQ and PTEQ, $N_r = 2$ receive antennas. 25

8 BER vs. decision delay d for TEQ and PTEQ, $N_r = 2$ receive antennas at $SNR = 15\ dB$. 26

9 BER vs. SNR for the PTEQ, when the true channel is used to design the equalizer. 27

LIST OF TABLES

I Implementation Complexity Comparison 17

Abstract

In this paper, we propose a time-domain as well as a frequency-domain per-tone equalization for OFDM over doubly-selective channels. We consider the most general case, where the channel delay spread is larger than the cyclic prefix (CP), which results into inter-block interference (IBI). IBI in conjunction with the Doppler effect destroys the orthogonality between subcarriers and hence, results into severe intercarrier interference (ICI). In this paper we propose a time-varying finite impulse response (TV-FIR) time-domain equalizer (TEQ) to restore the orthogonality between subcarriers and hence to eliminate ICI/IBI. Due to the fact that the TEQ optimizes the performance over all subcarriers in a joint fashion, it has a poor performance. An optimal frequency-domain per-tone equalizer (PTEQ) is then obtained by transferring the TEQ operation to the frequency-domain. Through computer simulations we demonstrate the performance of the proposed equalization techniques.

Index Terms

OFDM, Doubly-selective Channels, Basis Expansion Model (BEM), Time-domain Equalization, Per-tone Equalization.

I. INTRODUCTION

Orthogonal Frequency Division Multiplexing (OFDM) has attracted a lot of attention, due to its simple implementation and robustness against *frequency-selective* channels. In this paper, we consider OFDM transmission over *doubly-selective* (time- and frequency-selective) channels. In doubly-selective channels, the time variation of the channel over an OFDM block destroys the orthogonality between subcarriers and so induces intercarrier interference (ICI). In addition to this, inter-block interference (IBI) arises when the channel delay spread is larger than the cyclic prefix (CP), which again results into ICI. Hence, equalization techniques are required to restore the orthogonality and so to eliminate ICI/IBI. In this paper, we propose time-domain as well as frequency-domain per-tone equalization techniques to combat these channel effects. An emerging application that uses OFDM as a transmission technique is digital video broadcasting (DVB). DVB encounters long delay multipath channels. Using a CP of length equal to the channel order, results into a significant decrease in throughput. On the other hand, applying DVB over mobile channels for high speed terminals (motor way speeds) induces ICI which has been shown to decrease performance significantly. The motivation of this paper is to combat these channel effects for such applications.

Different approaches for reducing ICI have been proposed, including frequency-domain equalization and/or time-domain windowing. In [1], [2] the authors propose matched-filter, least-squares (LS) and minimum mean-square error (MMSE) receivers incorporating all subcarriers. Receivers considering the dominant adjacent subcarriers have been presented in [3], [4]. For multiple-input multiple-output (MIMO) OFDM over doubly-selective channels, a frequency-domain ICI mitigation technique is proposed in [5]. A time-domain windowing (linear pre-processing) approach to restrict ICI support in conjunction with iterative MMSE estimation is presented in [6]. ICI self-cancellation schemes are proposed in [7], [8]. There, redundancy is added to enable self-cancellation, which implies a substantial reduction in bandwidth efficiency. To avoid this rate loss, partial response encoding in conjunction with maximum-likelihood sequence detection to mitigate ICI in OFDM systems is studied in [9]. *However, all of*

the above mentioned works, assume the channel delay spread fits within the CP, and hence, no IBI is present. Moreover, in these works, the TV channel matrix (or an estimated version of it) is required to design the equalizer. This in return, requires a large number of parameters to be identified (tracked).

In this paper, we assume the channel delay spread is larger than the CP, and moreover, we approximate the TV channel by the basis expansion model (BEM). In this BEM, we assume that only the BEM coefficients are known at the receiver which is easier to obtain [10]. The BEM coefficients are then used to design the equalizer to equalize the true channel. In [11], [12], a frequency-domain ICI/IBI cancellation scheme is proposed for DMT systems without guard interval. The approach in the aforementioned articles depends on utilizing the nulled (unused) subcarriers to eliminate ICI/IBI, which is different than what we propose in this paper.

In [13], a time-invariant finite impulse response (TI-FIR) filter is applied to the time-domain received samples for OFDM transmission over frequency-selective channels whose delay spread is larger than the CP. The purpose of this time-domain equalizer (TEQ) is to shorten the channel delay-spread to fit within the CP. For the same problem an optimum frequency-domain per-tone equalizer (PTEQ) is proposed in [14]. The PTEQ is then obtained by transferring the TEQ operation to the frequency-domain.

Similarly, in this paper we apply a TV-FIR TEQ to convert the doubly-selective channel whose delay-spread is larger than the CP into a purely frequency-selective channel with a delay spread that fits within the CP. By doing this, we restore the orthogonality between subcarriers (eliminate IBI and ICI). Hence, an additional one-tap frequency-domain equalizer then allows us to estimate the QAM transmitted symbols. The proposed TV-FIR TEQ optimizes the performance on all subcarriers in a joint fashion. An optimum PTEQ is then obtained by transferring the TEQ operation to the frequency-domain. The proposed PTEQ optimizes the performance on each subcarrier separately.

The proposed techniques in this paper are different from those proposed in our earlier works: [16] for OFDM transmission over doubly-selective channels and [17] for single carrier transmission over doubly-selective channels.

- With respect to [16]:
  - i- In this work unlike [16], we assume the most general case, where the channel delay spread does not necessarily fit within the CP.
  - ii- The time-domain equalizer is assumed to be a multi-tap TV FIR filter instead of a one-tap TV filter as in [16]. This leads to a more general architecture, especially in the frequency-domain. This new architecture outperforms the one proposed in [16] (a gain of 3-dB is obtained for the SISO case). Moreover, this architecture allows us to approach the performance of the block MMSE equalizer (see Figure 6).
- With respect to [17]:
  - i- Single carrier transmission is considered in [17], whereas the current paper assumes OFDM.
  - ii- In [17] the channel delay spread fits within the CP.
  - iii- Only time-domain equalization is considered in [17], whereas in this paper we consider time- and frequency-domain equalization techniques.

iv- In [17] the BEM resolution is assumed to be equal to the window length. In the current work, we consider a BEM resolution that is an integer multiple of the window size. Increasing the BEM resolution (which corresponds to frequency-oversampling) results into a better fit when realistic fading channels are considered. Note that in [17], applying the proposed equalizer on a Jakes' channel results into a high error floor. This error floor is significantly reduced by frequency-oversampling as proposed in this paper. The fact that the BEM resolution is considered to be an integer multiple of the block size also leads to a more general architecture.

v- In [17], the time-domain equalizer is considered to completely equalize the channel, whereas in this work it requires to shorten the delay spread in order to fit within the CP and to remove the channel time variation. The latter design criterion gives more degrees of freedom.

This paper is organized as follows. In Section II, we present the system model. The basis expansion channel model is introduced in Section III. The proposed TEQ is presented in Section IV. In Section V, we introduce the PTEQ. An efficient implementation of the proposed PTEQ is discussed in Section VI. In Section VII, we show through computer simulations the performance of the proposed equalizer. Finally, our conclusions are drawn in Section VIII.

Notation: We use upper (lower) bold face letters to denote matrices (column vectors). Superscripts *, ^{T}, and ^{H} represent conjugate, transpose, and Hermitian, respectively. We denote the Kronecker delta as $\delta[n]$ and $\mathcal{E}\{\cdot\}$ denotes expectation. We use $\star$ to denote convolution. We denote the $N \times N$ identity matrix as $\mathbf{I}_N$, the $M \times N$ all-zero matrix as $\mathbf{0}_{M\times N}$ and the all ones vector of length M as $\mathbf{1}_M$. The kth element of vector $\mathbf{x}$ is denoted by $[\mathbf{x}]_k$. We denote $\mathbb{Z}^+$ the set of positive integers without zero. Finally, $\mathrm{diag}\{\mathbf{x}\}$ denotes the diagonal matrix with vector $\mathbf{x}$ on the diagonal, and $\mathrm{diag}\{\mathbf{A}_0, \ldots, \mathbf{A}_{M-1}\}$ denotes the block diagonal matrix with the submatrices $\mathbf{A}_0, \ldots, \mathbf{A}_{M-1}$ on the diagonal.

II. System Model

We assume a single-input multiple-output (SIMO) OFDM system (see Figure 1) with N_r receive antennas, but the results can be easily extended to multiple-input multiple-output (MIMO) systems. At the transmitter, the conventional OFDM modulation is applied, i.e., the incoming bit sequence is parsed into blocks of N frequency-domain QAM symbols. Each block is then transformed into a time-domain sequence using an N-point IDFT. A cyclic prefix (CP) of length ν is inserted at the head of each block. The time-domain blocks are then serially transmitted over a multipath fading channel. The channel is assumed to be time-varying (TV). Focusing only on the baseband-equivalent description, the received signal $y^{(r)}(t)$ at the rth receive antenna at time t, is given by:

$$y^{(r)}(t) = \sum_{n=-\infty}^{\infty} g^{(r)}(t; t-nT)x[n] + \eta^{(r)}(t),$$

where $g^{(r)}(t;\tau)$ is the baseband-equivalent of the doubly-selective channel from the transmitter to the rth receive antenna, $\eta^{(r)}(t)$ is the baseband-equivalent filtered additive noise at the rth receive antenna and $x[n]$ is the discrete time-domain sequence transmitted at a rate of $1/T$ symbols per second. Assuming $S_k[i]$ is the QAM symbol

transmitted on the kth subcarrier ($k \in \{0, \cdots, N-1\}$, N is the total number of subcarriers in the OFDM block) of the ith OFDM block, $x[n]$ can be written as:

$$x[n] = \frac{1}{\sqrt{N}} \sum_{k=0}^{N-1} S_k[i] e^{j2\pi(m-\nu)k/N},$$

where $i = \lfloor n/(N+\nu) \rfloor$ and $m = n - i(N+\nu)$. Note that this description includes the transmission of a CP of length ν.

The baseband-equivalent doubly-selective channel $g^{(r)}(t;\tau)$ includes the physical channel $g_{ch}^{(r)}(t;\tau)$ as well as the transmit filter $g_{tr}(t)$ and receive filter $g_{rec}(t)$:

$$g^{(r)}(t;\tau) = \int_{-\infty}^{\infty} \int_{-\infty}^{\infty} g_{rec}(s) g_{tr}(\tau - s - \theta) g_{ch}^{(r)}(t-s;\theta) \mathrm{d}s \mathrm{d}\theta.$$

Sampling each receive antenna at the symbol period T, the received sample sequence at the rth receive antenna $y^{(r)}[n] = y^{(r)}(nT)$, can be written as:

$$y^{(r)}[n] = \sum_{\theta=-\infty}^{\infty} g^{(r)}[n;\theta] x[n-\theta] + \eta^{(r)}[n], \tag{1}$$

where $\eta^{(r)}[n] = \eta^{(r)}(nT)$ and $g^{(r)}[n;\theta] = g^{(r)}(nT;\theta T)$.

Most wireless links experience multipath fading propagation due to scattering and reflection of the transmitted signal. Each resolvable path corresponds to a superposition of scattered rays that arrive at the receiver almost simultaneously with a common propagation delay, called a cluster. Each ray within the cluster is characterized by its own complex gain and Doppler shift. Hence, the physical channel $g_{ch}^{(r)}(t;\tau)$ can be written as [18], [19]:

$$g_{ch}^{(r)}(t;\tau) = \sum_{c} \delta(\tau - \tau_c^{(r)}) \sum_{\mu} G_{c,\mu}^{(r)} e^{j2\pi f_{c,\mu}^{(r)} t}, \tag{2}$$

where $\tau_c^{(r)}$ is the propagation delay of the cth cluster of the rth receive antenna, and $G_{c,\mu}^{(r)}$ and $f_{c,\mu}^{(r)}$ are the complex gain and the frequency offset respectively of the μth ray of the cth cluster characterizing the link between the transmitter and the rth receive antenna.

Assuming the time variation of the physical channel $g_{ch}^{(r)}(t;\tau)$ is negligible over the span of the receive filter $g_{rec}(t)$, we obtain:

$$\begin{aligned} g^{(r)}(t;\tau) &= \int_{-\infty}^{\infty} \left(\int_{-\infty}^{\infty} g_{rec}(s) g_{tr}(\tau - s - \theta) \mathrm{d}s \right) g_{ch}^{(r)}(t;\theta) \mathrm{d}\theta \\ &= \int_{-\infty}^{\infty} \psi(\tau - \theta) g_{ch}^{(r)}(t;\theta) \mathrm{d}\theta \\ &= \sum_{c} \psi(\tau - \tau_c^{(r)}) \sum_{\mu} G_{c,\mu}^{(r)} e^{j2\pi f_{c,\mu}^{(r)} t}. \end{aligned} \tag{3}$$

where $\psi(t) = g_{tr}(t) \star g_{rec}(t)$. Hence, we can express $g^{(r)}[n;\theta]$ as:

$$g^{(r)}[n;\theta] = \sum_{c} \psi(\theta T - \tau_c^{(r)}) \sum_{\mu} G_{c,\mu}^{(r)} e^{j2\pi f_{c,\mu}^{(r)} nT}.$$

The channel model described in (3) is a rather complex model, with a huge (possibly infinite) number of parameters to be identified/equalized. This motivates the use of an alternative channel model with fewer parameters.

In this paper, we use the basis expansion model (BEM) to approximate the discrete-time baseband-equivalent doubly-selective channel.

III. Basis Expansion Channel Model

In this section, we describe the BEM channel [20], [21], [22], [23]. In this BEM, the doubly-selective channel $g^{(r)}[n;\theta]$ is modeled as an FIR filter where the taps are expressed as a superposition of complex exponential basis functions with frequencies on a discrete grid. Assuming $g^{(r)}(t;\tau)=0$ for $\tau \notin [0,(L+1)T)$, each channel $g^{(r)}[n;\theta]$ can be approximated for $n \in \{i(N+\nu)+\nu+d-L', \ldots, (i+1)(N+\nu)+d-1\}$ (L' and d to be defined later) by a BEM (see Figure 2):

$$h^{(r)}[n;\theta] = \sum_{l=0}^{L} \delta[\theta-l] \sum_{q=-Q/2}^{Q/2} h_{q,l}^{(r)}[i] e^{j2\pi qn/K}, \tag{4}$$

where Q and K should be selected such that $Q/(KT) \geq 2f_{\max}$, with $f_{\max}$ the maximum Doppler spread of all channels:

$$f_{\max} = \max_{r,c,\mu} \{|f_{c,\mu}^{(r)}|\}.$$

In this expansion model, L represents the delay-spread (expressed in multiples of T, the delay resolution of the model), and $Q/2$ represents the Doppler-spread (expressed in multiples of $1/(KT)$, the Doppler resolution of the model). Note that the coefficients $h_{q,l}^{(r)}[i]$ remain invariant over a period of length $(N+L')T$, but may change from block to block.

Substituting (4) in (1), the received sample sequence at the rth receive antenna can be written as:

$$y^{(r)}[n] = \sum_{l=0}^{L} \sum_{q=-Q/2}^{Q/2} e^{j2\pi qn/K} h_{q,l}^{(r)}[i] x[n-l] + \eta^{(r)}[n]. \tag{5}$$

Not that in (4) and (5), due to the equalizer filter span L' (to be defined later), some overlap between consecutive blocks occurred. This overlap implies that some channel samples and received samples are defined twice, which may be inconsistent. Upon block processing of the received sequence, we take first the block index i, and accordingly we take $n \in \{i(N+\nu)+\nu+d-L', \ldots, (i+1)(N+\nu)+d-1\}$. Note that the definitions in (4) and (5) are merely approximations of the true channel and the received sequence respectively. These equations are used to simplify the derivation of the proposed equalizers (time-domain and frequency-domain), which are then used to equalize the true channel.

IV. Time-Domain Equalization

In this section, we introduce time-domain equalization (TEQ) for OFDM systems over doubly-selective channels. We assume the most general case, where the TV channel delay spread is larger than the CP. The TEQ is implemented by a TV-FIR filter, i.e., at the rth receive antenna, we apply a TV-FIR TEQ denoted by $w^{(r)}[n;\theta]$. The purpose of the TEQ is to convert the doubly-selective channel into a frequency-selective channel with a delay spread that fits within the CP. i.e. to convert the doubly-selective channel of order $L > \nu$ and $f_{\max} \neq 0$ into a target impulse response (TIR) $b[\theta]$ that is purely frequency-selective with order $L'' \leq \nu$ and $f_{\max} = 0$. The purpose of the TV-FIR

TEQ is thus to mitigate both IBI and ICI. As shown in Figure 3, we require to design a TV-FIR TEQ and TIR such that the difference term $e[n]$ is minimized in the mean square error sense, subject to some decision delay d.

The output of the TV-FIR TEQ at the rth receive antenna subject to some decision delay d, can be written as:

$$z^{(r)}[n] = \sum_{\theta=-\infty}^{\infty} w^{(r)}[n;\theta] y^{(r)}[n+d-\theta]. \tag{6}$$

Since we approximate the doubly-selective channel using the BEM, it is convenient to also model the TV-FIR TEQ using the BEM. In other words, we design the TV-FIR TEQ $w^{(r)}[n;\theta]$ to have $L'+1$ taps, where the time variation of each tap is modeled by $Q'+1$ time-varying complex exponential basis functions. Hence, we can write the TV-FIR TEQ $w^{(r)}[n;\theta]$ for $n \in \{i(N+\nu)+\nu, \cdots, (i+1)(N+\nu)-1\}$ as:

$$w^{(r)}[n;\theta] = \sum_{l'=0}^{L'} \delta[\theta - l'] \sum_{q'=-Q'/2}^{Q'/2} w^{(r)}_{q',l'}[i] e^{j2\pi q' n/K}. \tag{7}$$

Substituting (7) in (6) we obtain:

$$\begin{aligned} z^{(r)}[n] &= \sum_{l'=0}^{L'} \sum_{q'=-Q'/2}^{Q'/2} w^{(r)}_{q',l'}[i] e^{j2\pi q' n/K} y^{(r)}[n+d-l'] \\ &= \sum_{l'=0}^{L'} \sum_{q'=-Q'/2}^{Q'/2} \sum_{l=0}^{L} \sum_{q=-Q/2}^{Q/2} w^{(r)}_{q',l'}[i] h^{(r)}_{q,l}[i] e^{j2\pi q' n/K} e^{j2\pi q n/K} x[n+d-l-l'] \\ &\quad + \sum_{l'=0}^{L'} \sum_{q'=-Q'/2}^{Q'/2} w^{(r)}_{q',l'}[i] e^{j2\pi q' n/K} \eta^{(r)}[n+d-l']. \end{aligned} \tag{8}$$

It is more convenient at this point to switch to a block level formulation. Defining $\mathbf{z}^{(r)}[i] = [z^{(r)}[i(N+\nu)+\nu], \cdots, z^{(r)}[(i+1)(N+\nu)-1]]^T$, $\mathbf{x}[i] = [x[i(N+\nu)+\nu+d-L-L'], \cdots, x[(i+1)(N+\nu)+d-1]]^T$ and $\boldsymbol{\eta}^{(r)}[i] = [\eta^{(r)}[i(N+\nu)+d-L'], \cdots, \eta^{(r)}[(i+1)(N+\nu)+d-1]]^T$, then (8) on a block level can be formulated as:

$$\mathbf{z}^{(r)}[i] = \sum_{l'=0}^{L'} \sum_{q'=-Q'/2}^{Q'/2} \sum_{l=0}^{L} \sum_{q=-Q/2}^{Q/2} w^{(r)}_{q',l'}[i] h^{(r)}_{q,l}[i] \mathbf{D}_{q'}[i] \mathbf{Z}_{l'} \tilde{\mathbf{D}}_q[i] \tilde{\mathbf{Z}}_l \mathbf{x}[i] + \sum_{l'=0}^{L'} \sum_{q'=-Q'/2}^{Q'/2} w^{(r)}_{q',l'} \mathbf{D}_{q'}[i] \mathbf{Z}_{l'} \boldsymbol{\eta}[i], \tag{9}$$

where $\mathbf{D}_{q'}[i] = \mathrm{diag}\{[e^{j2\pi q'(i(N+\nu)+\nu)/K}, \ldots, e^{j2\pi q'((i+1)(N+\nu)-1)/K}]^T\}$, $\mathbf{Z}_{l'} = [\mathbf{0}_{N\times(L'-l')}, \mathbf{I}_N, \mathbf{0}_{N\times l'}]$, $\tilde{\mathbf{D}}_q[i] = \mathrm{diag}\{[e^{j2\pi q(i(N+\nu)+\nu-L')/K}, \ldots, e^{j2\pi q((i+1)(N+\nu)-1)/K}]^T\}$, and $\tilde{\mathbf{Z}}_l = [\mathbf{0}_{(N+L')\times(L-l)}, \mathbf{I}_{N+L'}, \mathbf{0}_{(N+L')\times l}]$. Using the property $\mathbf{Z}_{l'}\tilde{\mathbf{D}}_q[i] = e^{j2\pi q(L'-l')/K}\mathbf{D}_q[i]\mathbf{Z}_{l'}$, and defining $p = q+q'$ and $k = l+l'$, we can write (9) as:

$$\mathbf{z}[i] = \sum_{p=-(Q+Q')/2}^{(Q+Q')/2} \sum_{k=0}^{L+L'} f_{p,k}[i] \mathbf{D}_p[i] \bar{\mathbf{Z}}_k \mathbf{x}[i] + \sum_{r=1}^{N_r} \sum_{l'=0}^{L'} \sum_{q'=-Q'/2}^{Q'/2} w^{(r)}_{q',l'}[i] \mathbf{D}_{q'}[i] \mathbf{Z}_{l'} \boldsymbol{\eta}[i], \tag{10}$$

where $\mathbf{z}[i] = \sum_{r=1}^{N_r} \mathbf{z}^{(r)}[i]$, $\bar{\mathbf{Z}}_k = [\mathbf{0}_{N\times(L+L'-k)}, \mathbf{I}_N, \mathbf{0}_{N\times k}]$, and $f_{p,k}[i]$ can be written as:

$$f_{p,k}[i] = \sum_{r=1}^{N_r} \sum_{q'=-Q'/2}^{Q'/2} \sum_{l'=0}^{L'} e^{j2\pi(p-q')l'/K} w^{(r)}_{q',l'}[i] h^{(r)}_{p-q',k-l'}[i]. \tag{11}$$

Defining $\mathbf{f}[i] = [f_{-(Q+Q')/2,0}[i], \cdots, f_{(Q+Q')/2,L+L'}[i]]^T$, we can further write (10) as:

$$\begin{aligned}\mathbf{z}[i] &= (\mathbf{f}^T[i] \otimes \mathbf{I}_N)\mathbf{A}[i]\mathbf{x}[i] + \sum_{r=1}^{N_r} (\mathbf{w}^{(r)T}[i] \otimes \mathbf{I}_N)\mathbf{B}[i]\boldsymbol{\eta}^{(r)}[i] \\ &= (\mathbf{f}^T[i] \otimes \mathbf{I}_N)\mathbf{A}[i]\mathbf{x}[i] + (\mathbf{w}^T[i] \otimes \mathbf{I}_N)(\mathbf{I}_{N_r} \otimes \mathbf{B}[i])\boldsymbol{\eta}[i], \end{aligned} \tag{12}$$

where $\mathbf{w}^{(r)}[i] = [w^{(r)}_{-Q'/2,0}[i], \cdots, w^{(r)}_{Q'/2,L'}[i]]^T$, $\mathbf{w}[i] = [\mathbf{w}^{(1)T}[i], \cdots, \mathbf{w}^{(N_r)T}]^T[i]$, $\boldsymbol{\eta}[i] = [\boldsymbol{\eta}^{(1)T}[i], \cdots, \boldsymbol{\eta}^{(N_r)T}[i]]^T$, and $\mathbf{A}[i]$ and $\mathbf{B}[i]$ are given by:

$$\mathbf{A}[i] := \begin{bmatrix} \mathbf{D}_{-(Q+Q')/2}[i]\bar{\mathbf{Z}}_0 \\ \vdots \\ \mathbf{D}_{-(Q+Q')/2}[i]\bar{\mathbf{Z}}_{L+L'} \\ \vdots \\ \mathbf{D}_{(Q+Q')/2}[i]\bar{\mathbf{Z}}_{L+L'} \end{bmatrix}, \quad \mathbf{B} := \begin{bmatrix} \mathbf{D}_{-Q'/2}[i]\mathbf{Z}_0 \\ \vdots \\ \mathbf{D}_{-Q'/2}[i]\mathbf{Z}_{L'} \\ \vdots \\ \mathbf{D}_{Q'/2}[i]\mathbf{Z}_{L'} \end{bmatrix},$$

Note that the term in $f_{p,k}[i]$ corresponding to the rth receive antenna is related to a 2-dimensional convolution of the BEM coefficients of the doubly-selective channel for the rth receive antenna and the BEM coefficients of the TV-FIR TEQ for the rth receive antenna. This allows us to derive a linear relationship between $\mathbf{f}[i]$ and $\mathbf{w}[i]$. We first define the $(L'+1) \times (L'+L+1)$ Toeplitz matrix

$$\mathcal{T}_{l,L'+1}(h^{(r)}_{q,l}[i]) := \begin{bmatrix} h^{(r)}_{q,0}[i] & \dots & h^{(r)}_{q,L}[i] & & 0 \\ & \ddots & & \ddots & \\ 0 & & h^{(r)}_{q,0}[i] & \dots & h^{(r)}_{q,L}[i] \end{bmatrix}.$$

We then define $\boldsymbol{\mathcal{H}}^{(r)}_q[i] = \boldsymbol{\Omega}_q \mathcal{T}_{l,L'+1}(h^{(r)}_{q,l}[i])$, where $\boldsymbol{\Omega}_q = \mathrm{diag}\{[e^{j2\pi qL'/K}, \dots, 1]^T\}$, and introduce the $(Q'+1)(L'+1) \times (Q+Q'+1)(L+L'+1)$ block Toeplitz matrix

$$\mathcal{T}_{q,Q'+1}(\boldsymbol{\mathcal{H}}^{(r)}_q[i]) = \begin{bmatrix} \boldsymbol{\mathcal{H}}^{(r)}_{-Q/2}[i] & \dots & \boldsymbol{\mathcal{H}}^{(r)}_{Q/2}[i] & & \mathbf{0} \\ & \ddots & & \ddots & \\ \mathbf{0} & & \boldsymbol{\mathcal{H}}^{(r)}_{-Q/2}[i] & \dots & \boldsymbol{\mathcal{H}}^{(r)}_{Q/2}[i] \end{bmatrix}.$$

Introducing the definitions $\boldsymbol{\mathcal{H}}^{(r)}[i] = \mathcal{T}_{q,Q'+1}(\boldsymbol{\mathcal{H}}^{(r)}_q[i])$ and $\boldsymbol{\mathcal{H}}[i] = [\boldsymbol{\mathcal{H}}^{(1)T}[i], \dots, \boldsymbol{\mathcal{H}}^{(N_r)T}[i]]^T$, we can finally derive from (11) that:

$$\mathbf{f}^T[i] = \mathbf{w}^T[i]\boldsymbol{\mathcal{H}}[i]. \tag{13}$$

As already mentioned, the purpose of the TEQ is to convert the doubly-selective channel into a frequency-selective equivalent channel with order less than or equal the CP. To this aim, we define the so called target-impulse response (TIR) denoted by $b[\theta]$ and of order $L'' \leq \nu$, which can be modeled for $n \in \{i(N+\nu)+\nu, \dots, (i+1)(N+\nu)-1\}$ as:

$$b[\theta] = \sum_{l''=0}^{L''} \delta[\theta - l'']b_{l''}[i].$$

As shown in Figure 3, we will now design a TEQ $\mathbf{w}[i]$, a TIR $\mathbf{b}[i] = [b_0[i], \ldots, b_{L''}[i]]^T$ and a synchronization delay d such that the difference between the outputs of the upper branch and the lower branch is minimized. Defining $\mathbf{e}[i] = [e[i(N+\nu)], \ldots, e[i(N+\nu)+N-1]]^T$, we can express $\mathbf{e}[i]$ as:

$$\begin{aligned}\mathbf{e}[i] &= (\mathbf{f}^T[i] \otimes \mathbf{I}_N)\mathbf{A}[i]\mathbf{x}[i] + (\mathbf{w}^T[i] \otimes \mathbf{I}_N)(\mathbf{I}_{N_r} \otimes \mathbf{B}[i])\boldsymbol{\eta}[i] - \sum_{l''=0}^{L''} b_{l''}[i]\bar{\mathbf{Z}}_{l''}\mathbf{x}[i] \\ &= (\mathbf{f}^T[i] \otimes \mathbf{I}_N)\mathbf{A}[i]\mathbf{x}[i] + (\mathbf{w}^T[i] \otimes \mathbf{I}_N)(\mathbf{I}_{N_r} \otimes \mathbf{B}[i])\boldsymbol{\eta}[i] - (\tilde{\mathbf{b}}[i] \otimes \mathbf{I}_N)\mathbf{A}[i]\mathbf{x}[i] \qquad (14)\end{aligned}$$

where the augmented vector $\tilde{\mathbf{b}}[i]$ can be written as $\tilde{\mathbf{b}}[i] = \mathbf{C}\mathbf{b}[i]$ with the selection matrix $\mathbf{C}$ given by:

$$\mathbf{C} = \left[\begin{array}{c} \mathbf{0}_{((Q+Q')(L+L'+1)/2+d)\times(L''+1)} \\ \hline \mathbf{I}_{L''+1} \\ \hline \mathbf{0}_{((Q+Q')(L+L'+1)/2-L''-d-1)\times(L''+1)} \end{array}\right].$$

Hence, we can write the following cost function:

$$\begin{aligned}\mathcal{J}[i] &= \mathcal{E}\left\{\mathbf{e}^H[i]\mathbf{e}[i]\right\} \\ &= \mathrm{tr}\left\{(\mathbf{f}^T[i] \otimes \mathbf{I}_N)\mathbf{A}[i]\mathbf{R}_x\mathbf{A}^H[i](\mathbf{f}^*[i] \otimes \mathbf{I}_N)\right\} + \mathrm{tr}\left\{(\mathbf{w}^T[i] \otimes \mathbf{I}_N)(\mathbf{I}_{N_r} \otimes \mathbf{B}[i])\mathbf{R}_\eta(\mathbf{I}_{N_r} \otimes \mathbf{B}^H[i])(\mathbf{w}^*[i] \otimes \mathbf{I}_N)\right\} \\ &+ \mathrm{tr}\left\{(\tilde{\mathbf{b}}^T[i] \otimes \mathbf{I}_N)\mathbf{A}[i]\mathbf{R}_x\mathbf{A}^H[i](\tilde{\mathbf{b}}^*[i] \otimes \mathbf{I}_N)\right\} - 2\mathrm{tr}\left\{\Re\{(\mathbf{f}^T[i] \otimes \mathbf{I}_N)\mathbf{A}[i]\mathbf{R}_x\mathbf{A}^H[i](\tilde{\mathbf{b}}^*[i] \otimes \mathbf{I}_N)\}\right\} \qquad (15)\end{aligned}$$

Let us now introduce the following properties:

$$\begin{aligned}\mathrm{tr}\{(\mathbf{x}^T \otimes \mathbf{I}_N)\mathbf{X}(\mathbf{x}^* \otimes \mathbf{I}_N)\} &= \mathbf{x}^T\mathrm{subtr}\{\mathbf{X}\}\mathbf{x}^* \\ \mathrm{tr}\{(\mathbf{x}^T \otimes \mathbf{I}_N)\mathbf{V}(\mathbf{y}^* \otimes \mathbf{I}_N)\} &= \mathbf{x}^T\mathrm{subtr}\{\mathbf{V}\}\mathbf{y}^*,\end{aligned}$$

where subtr$\{\cdot\}$ splits the matrix up into $N \times N$ submatrices and replaces each submatrix by its trace [1]. Note that $\mathbf{X}$ is a square matrix while $\mathbf{V}$ is not necessarily square. Hence, subtr$\{\cdot\}$ reduces the row and column dimension by a factor N. Hence, the cost function in (15) reduces to:

$$\mathcal{J}[i] = \mathbf{w}^T[i]\left(\boldsymbol{\mathcal{H}}[i]\mathbf{R}_{\tilde{A}}[i]\boldsymbol{\mathcal{H}}^H[i] + \mathbf{R}_{\tilde{B}}[i]\right)\mathbf{w}^*[i] + \tilde{\mathbf{b}}^T[i]\mathbf{R}_{\tilde{A}}[i]\tilde{\mathbf{b}}^*[i] - 2\Re\{\mathbf{w}^T[i]\boldsymbol{\mathcal{H}}[i]\mathbf{R}_{\tilde{A}}[i]\tilde{\mathbf{b}}^*[i]\}, \qquad (16)$$

where $\mathbf{R}_{\tilde{A}}[i] = \mathrm{subtr}\{\mathbf{A}[i]\mathbf{R}_x\mathbf{A}^H[i]\}$, and $\mathbf{R}_{\tilde{B}}[i] = \mathrm{subtr}\left\{(\mathbf{I}_{N_r} \otimes \mathbf{B}[i])\mathbf{R}_\eta(\mathbf{I}_{N_r} \otimes \mathbf{B}^H[i])\right\}$. This cost function is now to be optimized w.r.t $\mathbf{w}[i]$ and $\mathbf{b}[i]$. In order to avoid the trivial solution (zero vector $\mathbf{w}[i]$ and zero vector $\mathbf{b}[i]$), non-triviality constraints need to be added. e.g., a unit tap constraint, $b_0[i] = 1$; a unit-norm constraint, $\|\mathbf{b}[i]\|^2 = 1$ or $\|\mathbf{w}[i]\|^2 = 1$; or a unit-energy constraint, $\mathbf{b}^H[i]\mathbf{R}_{\tilde{A}}[i]\mathbf{b}[i] = 1$ or $\mathbf{w}^H[i]\mathbf{R}_{\tilde{B}}[i]\mathbf{w}[i] = 1$. More details about these

[1] Let $\mathbf{A}$ be the $pN \times qN$ matrix: $\mathbf{A} = \begin{bmatrix} \mathbf{A}_{11} & \ldots & \mathbf{A}_{1q} \\ \vdots & \ddots & \vdots \\ \mathbf{A}_{p1} & \ldots & \mathbf{A}_{pq} \end{bmatrix}$, where $\mathbf{A}_{ij}$ is the (i,j)th $N \times N$ submatrix of $\mathbf{A}$. The $p \times q$ matrix subtr$\{\mathbf{A}\}$ is then given by: subtr$\{\mathbf{A}\} = \begin{bmatrix} \mathrm{tr}\{\mathbf{A}_{11}\} & \ldots & \mathrm{tr}\{\mathbf{A}_{1q}\} \\ \vdots & \ddots & \vdots \\ \mathrm{tr}\{\mathbf{A}_{p1}\} & \ldots & \mathrm{tr}\{\mathbf{A}_{pq}\} \end{bmatrix}$

constraints for TI channels can be found in [24] and [13] for the unit-tap and unit-norm constraints, and in [25] for the unit-energy constraint. A TEQ for the MIMO case is proposed in [26].

In this paper we only consider the unit norm constraint and the unit energy constraint for their superior performance to the other constraint (this is proven to be the case in DMT systems, and here is no exception):

a) Unit norm constraint: In this case we have the following optimization problem:

$$\min_{\mathbf{w}[i],\mathbf{b}[i]} \mathcal{J}[i] \text{ such that } \|\mathbf{b}[i]\|^2 = 1.$$

The solution to this problem is given by:

$$\mathbf{w}^T[i] = \tilde{\mathbf{b}}^T[i] \left(\boldsymbol{\mathcal{H}}^H[i]\mathbf{R}_{\tilde{B}}^{-1}[i]\boldsymbol{\mathcal{H}}[i] + \mathbf{R}_{\tilde{A}}^{-1}[i]\right)^{-1} \boldsymbol{\mathcal{H}}^H[i]\mathbf{R}_{\tilde{B}}^{-1}[i],$$
$$\mathbf{b}[i] = \text{eig}_{\min}(\mathbf{R}^{\perp}[i]),$$

where $\mathbf{R}^{\perp}[i]$ is given by:

$$\mathbf{R}^{\perp}[i] = \mathbf{C}^T \left(\boldsymbol{\mathcal{H}}^H[i]\mathbf{R}_{\tilde{B}}^{-1}[i]\boldsymbol{\mathcal{H}}[i] + \mathbf{R}_{\tilde{A}}^{-1}[i]\right)^{-1} \mathbf{C}$$

b) Unit energy constraint: In this case we have the following optimization problem:

$$\min_{\mathbf{w}[i],\mathbf{b}[i]} \mathcal{J}[i] \text{ such that } \tilde{\mathbf{b}}^H[i]\mathbf{R}_{\tilde{A}}[i]\tilde{\mathbf{b}}[i] = 1.$$

The solution to this optimization problem is given by:

$$\mathbf{w}^T[i] = \tilde{\mathbf{b}}^T[i] \left(\boldsymbol{\mathcal{H}}^H[i]\mathbf{R}_{\tilde{B}}^{-1}[i]\boldsymbol{\mathcal{H}}[i] + \mathbf{R}_{\tilde{A}}^{-1}[i]\right)^{-1} \boldsymbol{\mathcal{H}}^H[i]\mathbf{R}_{\tilde{B}}^{-1}[i],$$
$$\mathbf{b}[i] = \text{eig}_{\max}(\tilde{\mathbf{R}}^{\perp}[i]),$$

where $\tilde{\mathbf{R}}^{\perp}[i]$ is given by:

$$\tilde{\mathbf{R}}^{\perp}[i] = \mathbf{C}^T \left(\boldsymbol{\mathcal{H}}^H[i]\mathbf{R}_{\tilde{B}}^{-1}[i]\boldsymbol{\mathcal{H}}[i] + \mathbf{R}_{\tilde{A}}^{-1}[i]\right)^{-1} \boldsymbol{\mathcal{H}}^H\mathbf{R}_{\tilde{B}}^{-1}[i]\boldsymbol{\mathcal{H}}\mathbf{R}_{\tilde{A}}[i]\mathbf{C}.$$

Note that $\text{eig}_{\min}(\mathbf{A})$ ($\text{eig}_{\max}(\mathbf{A})$) is the eigenvector corresponding to the minimum (maximum) eigenvalue of the matrix $\mathbf{A}$.

In conjunction with the devised TEQ, a one-tap FEQ applied to the filtered received sequence in the frequency-domain is still necessary to fully recover the transmitted QAM symbols. Define $\hat{S}_k[i]$ as the estimate of the transmitted QAM symbol on the kth subcarrier of the ith OFDM symbol. This estimate is then obtained by applying a 1-tap FEQ to the TEQ output after the DFT-demodulation:

$$\hat{S}_k[i] = \frac{1}{d_k[i]} \mathcal{F}^{(k)} \sum_{r=1}^{N_r} \sum_{q'=-Q'/2}^{Q'/2} \mathbf{D}_{q'}[i]\mathbf{W}_{q'}^{(r)}[i]\mathbf{y}^{(r)}[i], \tag{17}$$

where $\mathcal{F}^{(k)}$ is the $(k+1)$st row of the FFT matrix $\boldsymbol{\mathcal{F}}$, $\mathbf{W}_{q'}^{(r)}[i]$ is an $N \times (N+L')$ Toeplitz matrix, with first column $[w_{q',L'}^{(r)}[i], \mathbf{0}_{1\times(N-1)}]^T$ and first row $[w_{q',L'}^{(r)}[i], \ldots, w_{q',0}^{(r)}[i], \mathbf{0}_{1\times(N-L'-1)}]$, $d_k[i]$ is the frequency response of the TIR on the kth subcarrier of the ith OFDM block ($1/d_k[i]$ represents the 1-tap FEQ), and $\mathbf{y}^{(r)}[i] = [y^{(r)}[i(N+\nu)+\nu+d-L'], \ldots, y^{(r)}[(i+1)(N+\nu)+d-1]]^T$.

The existence of a perfect shortening TEQ (a TEQ that completely eliminates IBI/ICI in the noiseless case) requires that $\boldsymbol{\mathcal{H}}$ is of full column rank. A necessary condition for $\boldsymbol{\mathcal{H}}$ to have full column rank is that $Nr(Q'+1)(L'+1) \geq (Q+Q'+1)(L+L'+1)$. For sufficiently large Q' and L', it is clear that we need at least two receive antennas, i.e. $N_r \geq 2$. This justifies our assumption of SIMO systems. Conditions like column reducedness and irreducibility can be deduced from the MIMO time-invariant FIR case. These are discussed in more detail in [17].

V. Frequency-Domain Per-Tone Equalization

In Section IV, a time-domain equalizer is proposed to combat the effect of the propagation channel. The purpose of the proposed TEQ is to convert the doubly-selective channel into a purely frequency-selective channel. The proposed TEQ optimizes the performance on all subcarriers in a joint fashion. An optimal frequency-domain per-tone equalizer (PTEQ) can be obtained by transferring the TEQ operations to the frequency-domain. Hence, the estimate of the transmitted QAM symbol on the kth subcarrier in the ith OFDM block is then obtained as:

$$\hat{S}_k[i] = \sum_{r=1}^{N_r} \sum_{q'=-Q'/2}^{Q'/2} \mathcal{F}^{(k)} \mathbf{D}_{q'}[i] \mathbf{Y}^{(r)}[i] \mathbf{w}_{q'}^{(r)}[i] / d_k[i] \tag{18a}$$

$$= \sum_{r=1}^{N_r} \sum_{q'=-Q'/2}^{Q'/2} \mathcal{F}^{(k)} \underbrace{\mathbf{D}_{q'}[i] \mathbf{Y}^{(r)}[i] \hat{\mathbf{D}}_{q'}^{*}}_{\tilde{\mathbf{Y}}_{q'}^{(r)}[i]} \underbrace{\hat{\mathbf{D}}_{q'} \mathbf{w}_{q'}^{(r)}[i] / d_k[i]}_{\tilde{\mathbf{w}}_{q'}^{(r,k)}[i]} \tag{18b}$$

where $\mathbf{Y}^{(r)}[i]$ is an $N \times (L'+1)$ Toeplitz matrix, with first column $[y^{(r)}[i(N+\nu)+\nu+d], \ldots, y^{(r)}[(i+1)(N+\nu)+d-1]]^T$ and first row $[y^{(r)}[i(N+\nu)+\nu+d], \ldots, y^{(r)}[i(N+\nu)+\nu+d-L']]$, $\mathbf{w}_{q'}^{(r)}[i] = [w_{q',0}^{(r)}[i], \ldots, w_{q',L'}^{(r)}[i]]^T$, and $\hat{\mathbf{D}}_{q'} = \mathrm{diag}\{[1, \ldots, e^{j2\pi q' L'/K}]^T\}$. Note that the right multiplication of $\mathbf{Y}^{(r)}[i]$ with the diagonal matrix $\hat{\mathbf{D}}_{q'}$ in (18b) is done here to restore the Toeplitz structure in $\mathbf{Y}_{q'}^{(r)}[i] = \mathbf{D}_{q'} \mathbf{Y}^{(r)}[i]$, which will simplify the analysis and implementation as will be clear later. From (18b), we can see that each subcarrier has its own $(L'+1)$-tap FEQ. This allows us to optimize the equalizer coefficients $\tilde{\mathbf{w}}_{q'}^{(r,k)}[i]$ for each subcarrier k separately, without taking into account the specific relation that existed originally between $\tilde{\mathbf{w}}_{q'}^{(r,k)}[i]$, $\mathbf{w}_{q'}^{(r,k)}[i]$, and $d_k[i]$.

Defining $\tilde{\mathbf{Y}}^{(r)}[i] = \left[\tilde{\mathbf{Y}}_{-Q'/2}^{(r)}[i], \ldots, \tilde{\mathbf{Y}}_{Q'/2}^{(r)}[i]\right]$ and $\tilde{\mathbf{w}}^{(r,k)}[i] = \left[\tilde{\mathbf{w}}_{-Q'/2}^{(r,k)T}[i], \ldots, \tilde{\mathbf{w}}_{Q'/2}^{(r,k)T}[i]\right]^T$, (18b) reduces to:

$$\hat{S}_k[i] = \sum_{r=1}^{N_r} \mathcal{F}^{(k)} \tilde{\mathbf{Y}}^{(r)}[i] \tilde{\mathbf{w}}^{(r,k)}[i]. \tag{19}$$

Transferring the TEQ operation to the frequency-domain by interchanging the TEQ with the DFT in (19), we obtain:

$$\hat{S}_k[i] = \sum_{r=1}^{N_r} \tilde{\mathbf{w}}^{(r,k)T}[i] \mathbf{F}^{(k)}[i] \mathbf{y}^{(r)}[i], \tag{20}$$

where $\mathbf{F}^{(k)}[i] = \left(\mathbf{I}_{Q'+1} \otimes \tilde{\boldsymbol{\mathcal{F}}}^{(k)}\right) \left[\tilde{\mathbf{D}}^T_{-Q'/2}[i], \ldots, \tilde{\mathbf{D}}^T_{Q'/2}[i]\right]^T$, and $\tilde{\boldsymbol{\mathcal{F}}}^{(k)}$ is given by:

$$\tilde{\boldsymbol{\mathcal{F}}}^{(k)} = \begin{bmatrix} 0 & \cdots & 0 & \boxed{\mathcal{F}^{(k)}} \\ \vdots & 0 & \boxed{\mathcal{F}^{(k)}} & 0 \\ 0 & \iddots & \iddots & 0 \\ \boxed{\mathcal{F}^{(k)}} & 0 & \cdots & 0 \end{bmatrix},$$

which corresponds to a sliding DFT operation, which will be implemented as a sliding FFT.

To compute (20), we require $(Q'+1)$ sliding FFTs per receive antenna. Each sliding FFT is applied to a modulated version of the sequence received on a particular antenna. The q'th sliding FFT on the rth receive antenna is shown in Figure 4. To estimate the transmitted QAM symbol on the kth subcarrier we then have to combine the outputs of the $N_r(Q'+1)$ PTEQs corresponding to the kth subcarrier. This results in a complexity of $(Q'+1)(L'+1)$ multiply-add (MA) operations per receive antenna per subcarrier, i.e., $N_r N(Q'+1)(L'+1)$ MA operations for a block of N symbols. In Section VI, we show how we can further reduce the complexity of the proposed PTEQ by replacing the $Q'+1$ sliding FFTs by only a few sliding FFTs, the number of which is entirely independent of Q' but rather depends on the BEM frequency resolution K. The removed sliding FFTs are compensated for by combining the PTEQ outputs of neighboring subcarriers on the remaining sliding FFTs.

In the following, we will show how the PTEQ coefficients can be computed in order to minimize the mean square error (MSE). Defining $\tilde{\mathbf{w}}^{(k)}[i] = [\tilde{\mathbf{w}}^{(1,k)T}[i], \ldots, \tilde{\mathbf{w}}^{(N_r,k)T}[i]]^T$ and $\mathbf{y}[i] = [\mathbf{y}^{(1)T}[i], \ldots, \mathbf{y}^{(N_r)T}[i]]^T$, (20) can be written as:

$$\hat{S}_k[i] = \tilde{\mathbf{w}}_k^T[i] \left(\mathbf{I}_{N_r} \otimes \mathbf{F}^{(k)}[i]\right) \mathbf{y}[i]. \tag{21}$$

At this point we may introduce a model for the received sequence on the rth receive antenna $\mathbf{y}^{(r)}[i]$ as:

$$\mathbf{y}^{(r)}[i] = \underbrace{\sum_{q=-Q/2}^{Q/2} \tilde{\mathbf{D}}_q[i] \left[\boldsymbol{O}_1, \mathbf{H}_q^{(r)}[i], \boldsymbol{O}_2\right] (\mathbf{I}_3 \otimes \mathbf{P}) \left(\mathbf{I}_3 \otimes \boldsymbol{\mathcal{F}}^H\right)}_{\mathbf{G}^{(r)}[i]} \underbrace{\begin{bmatrix} \mathbf{s}[i-1] \\ \mathbf{s}[i] \\ \mathbf{s}[i+1] \end{bmatrix}}_{\tilde{\mathbf{s}}} + \boldsymbol{\eta}^{(r)}[i], \tag{22}$$

where $\boldsymbol{O}_1 = \mathbf{0}_{(N+L')\times(N+2\nu+d-L-L')}$, $\boldsymbol{O}_2 = \mathbf{0}_{(N+L')\times(N+\nu-d)}$, $\mathbf{H}_q^{(r)}[i]$ is an $(N+L') \times (N+L'+L)$ Toeplitz matrix with first column $[h_{q,L}^{(r)}[i], \mathbf{0}_{1\times(N+L'-1)}]^T$ and first row $[h_{q,L}^{(r)}[i], \ldots, h_{q,0}^{(r)}[i], \mathbf{0}_{1\times(N+L'-L-1)}]$, and $\mathbf{P}$ is the CP insertion matrix given by:

$$\mathbf{P} = \begin{bmatrix} \mathbf{0}_{\nu\times(N-\nu)} & \mathbf{I}_\nu \\ & \mathbf{I}_N \end{bmatrix}.$$

To obtain the PTEQ coefficients for the kth subcarrier, we define the following mean-square error (MSE) cost function:

$$\mathcal{J}[i] = \mathcal{E}\left\{\left\|S_k[i] - \tilde{\mathbf{w}}^{(k)T}[i] \left(\mathbf{I}_{N_r} \otimes \mathbf{F}^{(k)}[i]\right) \mathbf{y}[i]\right\|^2\right\}$$

Hence, the minimum MSE (MMSE) PTEQ coefficients for the kth subcarrier are given by:

$$\tilde{\mathbf{w}}_{MMSE}^{(k)}[i] = \arg\min_{\tilde{\mathbf{w}}^{(k)}[i]} \mathcal{J}[i] \tag{23}$$

The solution of (23) is obtained by solving $\partial\mathcal{J}[i]/\partial\tilde{\mathbf{w}}^{(k)}[i]=\mathbf{0}$, which reduces to:

$$\tilde{\mathbf{w}}_{MMSE}^{(k)T}[i]=\left(\left(\mathbf{I}_{N_r}\otimes\mathbf{F}^{(k)}[i]\right)\left(\mathbf{G}[i]\mathbf{R}_{\tilde{s}}\mathbf{G}^H[i]+\mathbf{R}_\eta\right)\left(\mathbf{I}_{N_r}\otimes\mathbf{F}^{(k)H}[i]\right)\right)^{-1}\left(\mathbf{I}_{N_r}\otimes\mathbf{F}^{(k)}[i]\right)\mathbf{G}[i]\mathbf{R}_{\tilde{s}}\mathbf{e}^{(k)}, \quad (24)$$

where $\mathbf{G}[i]=[\mathbf{G}^{(1)T}[i],\ldots,\mathbf{G}^{(N_r)T}[i]]^T$ and $\mathbf{e}^{(k)}$ is the unit vector with a 1 in the position $N+k$.

Note that, in contrast to the time-domain approach, where the BEM resolution of the channel model and the BEM resolution of the TV-FIR TEQ are assumed to be equal, the BEM resolution of the channel model and the BEM resolution of the PTEQ can be different.

VI. Efficient Implementation of the PTEQ

In Section V, we have shown that to implement the proposed PTEQ, we basically require $(Q'+1)$ sliding FFTs. In this section, we show how we can lower the complexity of the proposed PTEQ by further exploiting the special structure of $\tilde{\mathbf{Y}}_{q'}^{(r)}[i]$ (see (18b)). Our complexity reduction will proceed in two steps:

Step 1**:** In general, the BEM frequency resolution K is greater than or equal to the DFT size N. We will assume that K is an integer multiple of the FFT size, i.e., $K=PN$, where P is an integer greater than or equal to 1 ($P\in\mathbb{Z}^+$). We start by defining $\mathbb{Q}=\{-Q'/2,\ldots,Q'/2\}$, and $\mathbb{Q}_p=\{q\in\mathbb{Q}\mid q \mod P=p\}$. Based on these definitions, (18b) and (19) can be written as:

$$\hat{S}_k[i]=\sum_{r=1}^{N_r}\sum_{p=0}^{P-1}\sum_{q_p\in\mathbb{Q}_p}\mathcal{F}^{(k-l_p)}\underbrace{\mathbf{D}_p[i]\mathbf{Y}^{(r)}[i]\hat{\mathbf{D}}_p^*}_{\tilde{\mathbf{Y}}_p^{(r)}[i]}\underbrace{\hat{\mathbf{D}}_p\mathbf{w}_{p,l_p}^{(r,k)}[i]/d_k[i]}_{\bar{\mathbf{w}}_{p,l_p}^{(r,k)}[i]} \quad (25a)$$

$$=\sum_{r=1}^{N_r}\sum_{p=0}^{P-1}\sum_{q_p\in\mathbb{Q}_p}\mathcal{F}^{(k-l_p)}\tilde{\mathbf{Y}}_p^{(r)}[i]\bar{\mathbf{w}}_{p,l_p}^{(r,k)}[i], \quad (25b)$$

where $l_p=\frac{q_p-p}{P}$, and $\mathbf{w}_{p,l_p}^{(r,k)}[i]=\mathbf{w}_{q_p}^{(r,k)}[i]$. Note that (25b) splits the $Q'+1$ different terms of (19) into P different groups, with the pth group containing $|\mathbb{Q}_p|$ terms, where $|\mathbb{Q}_p|$ denotes the cardinality of the set $\mathbb{Q}_p$ for $p=0,\ldots,P-1$. Transferring the TEQ operation to the frequency-domain, we obtain:

$$\hat{S}_k[i]=\sum_{r=1}^{N_r}\sum_{p=0}^{P-1}\sum_{q_p\in\mathbb{Q}_p}\bar{\mathbf{w}}_{p,l_p}^{(r,k)T}[i]\tilde{\boldsymbol{\mathcal{F}}}^{(k-l_p)}\underbrace{\tilde{\mathbf{D}}_p[i]\mathbf{y}^{(r)}[i]}_{\tilde{\mathbf{y}}_p^{(r)}[i]} \quad (26)$$

Note that $\tilde{\mathbf{y}}_p^{(r)T}[i]=[\tilde{y}_p^{(r)}[i(N+\nu)+\nu+d-L'],\ldots,\tilde{y}_p^{(r)}[(i+1)(N+\nu)+d-1]]^T$ with $\tilde{y}_p^{(r)}[n]=e^{j2\pi pn/K}y^{(r)}[n]$, which is the pth modulated version of the received sequence.

Defining $\bar{\mathbf{w}}_p^{(r,k)}[i]=[\ldots,\bar{\mathbf{w}}_{p,-1}^{(r,k)T}[i],\bar{\mathbf{w}}_{p,0}^{(r,k)T}[i],\bar{\mathbf{w}}_{p,1}^{(r,k)T}[i],\ldots]^T$, (26) can now be written as:

$$\hat{S}_k[i]=\sum_{r=1}^{N_r}\sum_{p=0}^{P-1}\bar{\mathbf{w}}_p^{(r,k)T}[i]\tilde{\mathbf{F}}_p^{(k)}\tilde{\mathbf{y}}_p^{(r)}[i] \quad (27)$$

where $\tilde{\mathbf{F}}_p^{(k)}=[\ldots,\tilde{\boldsymbol{\mathcal{F}}}^{(k-1)T},\tilde{\boldsymbol{\mathcal{F}}}^{(k)T},\tilde{\boldsymbol{\mathcal{F}}}^{(k+1)T},\ldots]^T$. Let us now define $\tilde{\mathbf{F}}^{(k)}=\operatorname{diag}\left\{\tilde{\mathbf{F}}_0^{(k)T},\ldots,\tilde{\mathbf{F}}_{P-1}^{(k)T}\right\}$, $\tilde{\mathbf{y}}^{(r)}[i]=[\tilde{\mathbf{y}}_0^{(r)T}[i],\ldots,\tilde{\mathbf{y}}_{P-1}^{(r)T}[i]]^T$ and $\tilde{\mathbf{y}}[i]=[\tilde{\mathbf{y}}^{(1)T}[i],\ldots,\tilde{\mathbf{y}}^{(N_r)T}[i]]^T$. Further defining $\bar{\mathbf{w}}^{(r,k)}[i]=[\bar{\mathbf{w}}_0^{(r,k)T}[i],\ldots,\bar{\mathbf{w}}_{P-1}^{(r,k)T}[i]]^T$ and $\bar{\mathbf{w}}^{(k)}[i]=[\bar{\mathbf{w}}^{(1,k)T}[i],\ldots,\bar{\mathbf{w}}^{(N_r,k)T}[i]]^T$, (27) can finally be written as:

$$\hat{S}_k[i]=\bar{\mathbf{w}}^{(k)T}[i](\mathbf{I}_{N_r}\otimes\tilde{\mathbf{F}}^{(k)})\tilde{\mathbf{y}}[i] \quad (28)$$

To implement (27), we require P sliding FFTs per receive antenna rather than $Q'+1$ sliding FFTs per receive antenna as in Section V (in practice and in our simulations $P \ll Q'+1$). Each sliding FFT is applied to a modulated version of the received sequence. This reduction in the number of sliding FFTs per receive antenna is compensated for by combining $|\mathbb{Q}_p|$ neighboring subcarriers on the pth sliding FFT. Notice here that apart from the reduction in the number of sliding FFTs, the implementation complexity remains the same as in Section V, i.e., $N_r N(Q'+1)(L'+1)$ MA operations for a block of N symbols.

Similar to (23), we can construct the MSE cost function as:

$$\mathcal{J}[i] = \mathcal{E}\left\{\left\| S_k[i] - \bar{\mathbf{w}}^{(k)T}[i]\left(\mathbf{I}_{N_r} \otimes \tilde{\mathbf{F}}^{(k)}\right)\tilde{\mathbf{y}}[i]\right\|^2\right\} \tag{29}$$

The solution of (29) is:

$$\bar{\mathbf{w}}^{(k)T}_{MMSE}[i] = \left(\left(\mathbf{I}_{N_r} \otimes \tilde{\mathbf{F}}^{(k)}[i]\right)\left(\mathbf{G}[i]\mathbf{R}_{\tilde{s}}\mathbf{G}^H[i] + \mathbf{R}_\eta\right)\left(\mathbf{I}_{N_r} \otimes \tilde{\mathbf{F}}^{(k)H}[i]\right)\right)^{-1}\left(\mathbf{I}_{N_r} \otimes \tilde{\mathbf{F}}^{(k)}[i]\right)\mathbf{G}[i]\mathbf{R}_{\tilde{s}}\mathbf{e}^{(k)}, \tag{30}$$

which is equivalent to the one obtained in (24).

Step 2: We can further simplify the computational complexity associated with the proposed PTEQ by replacing each sliding FFT by only one full FFT and L' difference terms that are common to all subcarriers similar to the procedure in [27]. To explain this, we will consider only one sliding FFT. Let us consider the kth subcarrier of the pth sliding FFT, i.e., $\tilde{\boldsymbol{\mathcal{F}}}^{(k)}\tilde{\mathbf{y}}_p^{(r)}[i]$. Define $\tilde{Y}_p^{(r,k)} = \mathcal{F}^{(k)}[\tilde{y}_p^{(r)}[i(N+\nu)+\nu+d], \ldots, \tilde{y}_p^{(r)}[(i+1)(N+\nu)+d-1]]^T$ as the frequency response on the kth subcarrier of the pth modulated version of the received sequence on the rth receive antenna. It can then be shown that:

$$\tilde{\boldsymbol{\mathcal{F}}}^{(k)}\tilde{\mathbf{y}}_p^{(r)}[i] = \mathbf{T}^{(k)}\begin{bmatrix}\tilde{Y}_p^{(r,k)} \\ \Delta\tilde{\mathbf{y}}_p^{(r)}[i]\end{bmatrix}\begin{matrix}\updownarrow 1 \times 1 \\ \updownarrow L' \times 1\end{matrix}, \tag{31}$$

where $\mathbf{T}^{(k)}$ is an $(L'+1)\times(L'+1)$ lower triangular Toeplitz matrix given by:

$$\mathbf{T}^{(k)} = \begin{bmatrix} 1 & 0 & \cdots & 0 \\ \beta^k & \ddots & \ddots & \vdots \\ \vdots & \ddots & \ddots & 0 \\ \beta^{kL'} & \cdots & \beta^k & 1 \end{bmatrix}, \tag{32}$$

with $\beta = e^{-j2\pi/N}$. The difference terms $\Delta\tilde{\mathbf{y}}_p^{(r)}[i]$ are given by:

$$\Delta\tilde{\mathbf{y}}_p^{(r)}[i] = \begin{bmatrix} \tilde{y}_p^{(r)}[i(N+\nu)+\nu+d-1] - \tilde{y}_p^{(r)}[(i+1)(N+\nu)+d-1] \\ \vdots \\ \tilde{y}_p^{(r)}[i(N+\nu)+\nu+d-L'] - \tilde{y}_p^{(r)}[(i+1)(N+\nu)+d-L'-1] \end{bmatrix}.$$

In a similar fashion, we can obtain an expression for the neighboring subcarriers on the same sliding FFT by replacing the subcarrier index. The symbol estimate (28) can then be written as follows. We first define $\mathbf{u}_{p,l_p}^{(r,k)T}[i] = \bar{\mathbf{w}}_{p,l_p}^{(r,k)T}[i]\mathbf{T}^{(k+l_p)}$ and also define the following $|\mathbb{Q}_p|(L'+1)\times(|\mathbb{Q}_p|+L')$ selection matrix:

$$\mathbf{S}_p = \tilde{\mathbf{I}} \otimes \begin{bmatrix} 1 \\ \mathbf{0}_{L'\times 1} \end{bmatrix} + \begin{bmatrix} \mathbf{0}_{1\times(|\mathbb{Q}_p|+L')} \\ \tilde{\tilde{\mathbf{I}}} \end{bmatrix} \otimes \mathbf{1}_{|\mathbb{Q}_p|},$$

where $\tilde{\mathbf{I}}$ is the first $|\mathbb{Q}_p|$ rows of the matrix $\mathbf{I}_{|\mathbb{Q}_p|+L'}$, and $\tilde{\tilde{\mathbf{I}}}$ is the last L' rows of the matrix $\mathbf{I}_{|\mathbb{Q}_p|+L'}$. Introducing $\mathbf{u}_p^{(r,k)T}[i] = [\dots, \mathbf{u}_{p,-1}^{(r,k)T}[i], \mathbf{u}_{p,0}^{(r,k)T}[i], \mathbf{u}_{p,1}^{(r,k)T}[i], \dots]^T$ and $\mathbf{v}_p^{(r,k)T}[i] = \mathbf{u}_p^{(r,k)T}[i]\mathbf{S}_p$, (28) can then be written as:

$$\hat{S}_k[i] = \sum_{r=1}^{N_r}\sum_{p=0}^{P-1} \mathbf{v}_p^{(r,k)T}[i] \left[\begin{array}{c} \vdots \\ \tilde{Y}_p^{(r,k-1)}[i] \\ \tilde{Y}_p^{(r,k)}[i] \\ \tilde{Y}_p^{(r,k+1)}[i] \\ \vdots \\ \hline \Delta\tilde{\mathbf{y}}_p^{(r)}[i] \end{array}\right] \begin{array}{l} \updownarrow |\mathbb{Q}_p| \times 1 \\ \\ \\ \\ \\ \updownarrow L' \times 1 \end{array}$$

$$= \sum_{r=1}^{N_r}\sum_{p=0}^{P-1} \mathbf{v}_p^{(r,k)T}[i] \underbrace{\left[\begin{array}{cc} \vdots & \vdots \\ \mathbf{0}_{1\times L'} & \mathcal{F}^{(k-1)} \\ \mathbf{0}_{1\times L'} & \mathcal{F}^{(k)} \\ \mathbf{0}_{1\times L'} & \mathcal{F}^{(k+1)} \\ \vdots & \vdots \\ \hline \bar{\mathbf{I}}_{L'} & \mathbf{0}_{L'\times(N-L')} \quad -\bar{\mathbf{I}}_{L'} \end{array}\right]}_{\tilde{\mathbf{F}}_p^{(k)}} \tilde{\mathbf{y}}_p^{(r)}[i], \tag{33}$$

where $\bar{\mathbf{I}}_{L'}$ is the anti-diagonal identity matrix of size $L' \times L'$. Defining $\mathbf{v}^{(r,k)}[i] = [\mathbf{v}_0^{(r,k)T}[i], \dots, \mathbf{v}_{P-1}^{(r,k)T}[i]]^T$, $\mathbf{v}^{(k)}[i] = [\mathbf{v}^{(1,k)T}[i], \dots, \mathbf{v}^{(N_r,k)T}[i]]^T$ and $\tilde{\mathbf{F}} = \mathrm{diag}\{\tilde{\mathbf{F}}_0^T, \dots, \tilde{\mathbf{F}}_P^T\}$, (33) can finally be written as:

$$\hat{S}_k = \mathbf{v}^{(k)T}[i](\mathbf{I}_{N_r} \otimes \tilde{\mathbf{F}}^{(k)})\tilde{\mathbf{y}}[i]. \tag{34}$$

Note that, due to the fact that the difference terms are common to all subcarriers in a particular sliding FFT, the implementation complexity is $P(L'+1)+Q'+1$ MA operations per receive antenna per subcarrier, compared to $(Q'+1)(L'+1)$ per receive antenna per subcarrier in Section V. In Figure 5, we show how (34) can be realized for the pth sliding FFT on the rth receive antenna. Note that replacing the sliding FFT with one full DFT and L' difference terms in Section V, will not reduce the implementation complexity. This is due to the fact that we only consider a single subcarrier output for each sliding FFT to estimate a particular symbol. The implementation complexity of the TEQ and the different configurations of the PTEQ is summarized in Table I[2]. On the other hand, the design complexity of the PTEQ is higher than the design complexity of the TEQ. We can easily show that the design complexity of the TEQ requires $\mathcal{O}\big((Q+Q'+1)^3(L+L'+1)^3\big)$ multiply-add (MA) operations, while it requires $\mathcal{O}\left((Q'+1)(L'+1)N\right)$ MA operations per subcarrier to design the PTEQs. The design complexity of the TEQ is mainly due to a matrix inversion of size $(Q+Q'+1)(L+L'+1) \times (Q+Q'+1)(L+L'+1)$. The complexity associated with computing the $\max$ ($\min$) eigenvector of an $(L''+1)\times(L''+1)$ matrix which requires $\mathcal{O}\left((L''+1)^2\right)$ MA operations [28], is negligible compared to the above matrix inversion.

[2]These figures does not take into account the BEM channel coefficients estimation/computation.

TABLE I

IMPLEMENTATION COMPLEXITY COMPARISON

	MA/tone/rx	FFT/rx
TEQ	$(Q'+1)(L'+1)+1$	1
PTEQ (Figure 4)	$(Q'+1)(L'+1)$	$(Q'+1)$ sliding FFTs
PTEQ (Figure 5)	$P(L'+1)+Q'+1$	P FFTs

We finally note that our approach unifies and extends many existing frequency-domain approaches, for the case of TI as well as TV channels as follows:

i- TI Channels ($Q=0$, and hence $Q'=0$):

a) $\nu \geq L$, and $L'=0$: the proposed PTEQ comes down to the 1-tap MMSE FEQ as in [29].

b) $\nu < L$, and $L' \neq 0$: the proposed PTEQ comes down to the per-tone equalizer proposed in [14] for DMT-based transmission (e.g., for DSL modems).

ii- TV Channels ($Q' \neq 0$):

a) $\nu \geq L$, $L'=0$, and $P=1$: the proposed PTEQ comes down to the FEQ proposed in [4].

b) $\nu \geq L$, $L'=0$, and $P \geq 1$: the proposed PTEQ comes down to the FEQ proposed in [15].

VII. SIMULATIONS

In this section, we show some simulation results for the proposed IBI/ICI mitigation techniques. We consider a SISO system as well as a SIMO system with $N_r=2$ receive antennas. The channel is assumed to be doubly-selective of order $L=6$ with a maximum Doppler frequency of $f_{\max}=100Hz$ (corresponds to a speed of $120Km/hr$ on the GSM band of $900MHz$). The channel taps are simulated as i.i.d., correlated in time with a correlation function according to Jakes' model $\mathcal{E}\{h^{(r)}[n_1;l_1]h^{(r')*}[n_2;l_2]\}=\sigma_h^2 J_0(2\pi f_{\max}T(n_1-n_2))\delta[l_1-l_2]\delta[r-r']$, where J_0 is the zeroth-order Bessel function of the first kind and σ_h^2 denotes the variance of the channel. We consider an OFDM transmission with $N=128$ subcarriers. QPSK signaling is assumed. The sampling time is $T=50\mu sec$ which corresponds to a data rate of $40kbps$, which is suitable for applications like mobile multimedia (M^3). The normalized Doppler frequency is then obtained as $f_{\max}T=0.005$. We define the SNR as $SNR=\sigma_h^2(L+1)E_s/\sigma_\eta^2$, where E_s is the QPSK symbol power. The decision delay d is always chosen as $d=\lfloor (L+L')/2 \rfloor+1$.

We use a BEM to approximate the channel. We assume that the BEM coefficients are known at the receiver (obtained through an LS fit of the true channel in the noiseless case). The BEM coefficients of the approximated channel are used to design the time-domain and the frequency-domain per-tone equalizers. These equalizers, however, are used to equalize the true channel (Jakes' model). The BEM resolution is determined by $K=PN$ with P is chosen as $P=1,2$. The number of TV basis functions of the channel is chosen such that $Q/(2KT) \geq f_{\max}$ is satisfied, which results into $Q=2$ for $P=1$, and $Q=4$ for $P=2$.

• First, we consider a SISO system, where the channel impulse response fits within the CP, i.e., $\nu = L$. Hence, the total OFDM symbol duration is $6.7\ msec$. We measure the performance in terms of the BER vs. SNR. We consider a TEQ with $Q' = 14$, $L' = 14$ and $P = 2$. We consider the unit energy constraint (UEC), and the unit norm constraint (UNC). For the PTEQ, we use different scenarios. More specifically, we consider a PTEQ resulting from:

- a purely time-selective TEQ with $Q' = 10$ and $L' = 0$, and $P = 1$ as in [16].
- a purely time-selective TEQ with $Q' = 10$ and $L' = 0$, and $P = 2$ as in [16].
- a doubly-selective TEQ with $Q' = 10$ and $L' = 6$, and $P = 1$.
- a doubly-selective TEQ with $Q' = 10$ and $L' = 6$, and $P = 2$.

As a benchmark, we consider the case of OFDM transmission over purely frequency-selective (TI) channels where the equalizer is the conventional 1-tap MMSE FEQ, as well as OFDM transmission over doubly-selective (TV) channels with a block MMSE equalizer. The block MMSE equalizer for OFDM used here is similar to the block MMSE proposed in [17] designed for single carrier (SC) transmission with CP. As shown in Figure 6, the performance of the TEQ suffers from an early error floor for both UEC and UNC. The PTEQ exhibits a similar performance when $P = 1$ for both $L' = 0$ and $L' = 6$. However, the performance of the PTEQ is significantly improved when $P = 2$. For $P = 2$ with $L' = 0$, we see that the PTEQ slightly outperforms the 1-tap MMSE equalizer for OFDM over TI channels for low SNR ($SNR \leq 20\ dB$), and it experiences a $3\ dB$ loss in SNR compared to the block MMSE for OFDM over TV channels. On the other hand, when $P = 2$ with $L' = 6$, the PTEQ outperforms the conventional 1-tap MMSE FEQ of OFDM over TI channels, with an SNR gain of $2\ dB$ at $BER = 10^{-2}$, and coincides with the performance of the block MMSE equalizer for OFDM over TV channels.

• Second, we consider a SIMO system with $N_r = 2$ receive antennas. We consider the case where the cyclic prefix ν is shorter than the channel order, ν is chosen to be $\nu = 3$. The OFDM symbol duration is then $6.55\ msec$. We consider a TEQ with $Q' = 8$ and $L' = 8$. A PTEQ is then obtained by transferring this TEQ to the frequency-domain. We consider the case when $P = 1$ and $P = 2$. As shown in Figure 7, both the TEQ and the PTEQ suffers from an early error floor when $P = 1$, where the first exhibits an error floor at $BER = 4 \times 10^{-2}$ and $SNR = 20\ dB$ and the latter at $BER = 10^{-2}$ and $SNR = 20\ dB$. The performance is significantly improved when $P = 2$ for both the TEQ and the PTEQ. The PTEQ significantly outperforms the TEQ, where we can see a $6\ dB$ gain in SNR for the PTEQ over the TEQ at $BER = 10^{-2}$. The TEQ experiences a $4\ dB$ loss in SNR compared to the 1-tap MMSE FEQ for OFDM over TI channels, and $6\ dB$ loss in SNR compared to the PTEQ which coincides with the block MMSE for OFDM over TV channels.

• Third, we examine the effect of the decision delay d on the BER performance for the TEQ considering the UEC and UNC, and the PTEQ. We consider again the cases $P = 1$ and $P = 2$ for a SIMO system with $N_r = 2$ receive antennas and the same equalizer parameters as before. We examine the performance at $SNR = 15\ dB$. As shown in Figure 8, the performance of the PTEQ approach is a much smoother function of the synchronization delay than the performance of the TEQ approach. Hence, for the PTEQ approach the synchronization delay setting

is less critical than for the TEQ approach.

• In our setup so far we use the BEM coefficients (i.e., the approximated channel) to design the PTEQ. Here, we consider the performance of the PTEQ when the true channel is used for equalizer designs as well as evaluations. The channel is assumed to be a doubly-selective channel with maximum Doppler frequency $f_{\max} = 100\ Hz$, and sampling time $T = 50\ \mu sec$. The channel order is assumed to be $L = 6$. We consider a SISO system as well as a SIMO system with $N_r = 2$ receive antennas. For both cases we consider an OFDM transmission with $N = 128$ subcarriers and a cyclic prefix of length $\nu = 3$. We examine the performance of the PTEQ for $P = 1$ and $P = 2$. For the SISO system, the equalizer parameters are chosen as: $Q' = 4$ and $L' = 10$ for $P = 1$ and $Q' = 8$ and $L' = 10$ for $P = 2$. For the SIMO system, the equalizer parameters are chosen as: $Q' = 2$ and $L' = 8$ for $P = 1$ and $Q' = 4$ and $L' = 8$ for $P = 2$. Note that, in order to keep the same subcarrier span, the Q' for $P = 2$ is chosen to be twice as large as the Q' for $P = 1$. As shown in Figure 9, the PTEQ with $P = 2$ outperforms the PTEQ with $P = 1$ for the same subcarrier span. For the SISO case, an SNR gain of $4\ dB$ is obtained for the PTEQ with $P = 2$ over the PTEQ with $P = 1$ at $BER = 10^{-2}$. Similarly, an SNR gain of $2\ dB$ is obtained for the PTEQ with $P = 2$ over the PTEQ with $P = 1$ at $BER = 10^{-2}$ for the SIMO case.

VIII. Conclusions

In this paper, we propose a time-domain (TEQ) and a frequency-domain per-tone equalizer (PTEQ) for OFDM over doubly-selective channels. We consider the most general case where the channel delay spread is larger than the CP. The TV channel is approximated using the BEM. The TEQ is implemented as a TV-FIR filter. We use a BEM to model the TV-FIR TEQ. The PTEQ is then obtained by transferring the TEQ operation to the frequency-domain. Comparing the TEQ to the PTEQ we arrive at the following conclusions[3]:

- While the TEQ optimizes the performance on all subcarriers in a joint fashion, the PTEQ optimizes the performance on each subcarrier separately, leading to improved performance.
- The design complexity of the PTEQ is higher than the design complexity of the TEQ.
- The implementation complexity of the PTEQ is comparable to the implementation complexity of the TEQ (apart from the fact that the PTEQ may require additional FFTs).

From the simulations we arrive at the following conclusions:

- The PTEQ always outperforms the TEQ.
- The PTEQ is less sensitive to the choice of the decision delay.
- A key role in the performance of the TEQ and PTEQ is the BEM frequency resolution. We show that a BEM resolution equal to twice the DFT resolution (the DFT size) is enough to get an acceptable performance.
- The PTEQ outperforms the conventional 1-tap FEQ for OFDM over TI channels.
- The PTEQ approaches the performance of the block MMSE equalizer for OFDM over doubly-selective channels.

[3]Note that some of these conclusions are analogous to the results obtained for the time-invariant case.

- Oversampling the received sequence while keeping the same ICI span pays off.

REFERENCES

[1] Y.-S. Choi, P. J. Voltz, and F. A. Cassara, "On Channel Estimation and Detection for Multicarrier Signals in Fast and Selective Rayleigh Fading Channels," *IEEE Trans. Commun.*, vol. 49, pp. 1375–1387, Aug. 2001.

[2] W. G. Jeon, K. H. Chang, and Y. S. Cho, "An Equalization Technique for Orthogonal Frequency Division Multiplexing Systems in Time-Variant Multipath Channels," *IEEE Trans. Commun.*, vol. 47, pp. 27–32, Jan. 1999.

[3] X. Cai and G. B. Giannakis, "Low-Complexity ICI Suppression for OFDM over Time- and Frequency-Selective Rayleigh Fading Channels," in *Proc. of 36th Asilomar Conf. on Signals, Systems, and Computers*, (Pacific Grove, CA), pp. 1822–1826, Nov. 2002.

[4] X. Cai and G. B. Giannakis, "Bounding Performance and Suppressing Inter-Carrier Interference in Wireless Mobile OFDM," *IEEE Trans. Commun.*, pp. 2047 – 2056, Dec. 2003.

[5] A. Stamoulis, S. N. Diggavi, and N. Al-Dhahir, "Intercarrier Interference in MIMO OFDM," *IEEE Trans. Signal Processing*, vol. 50, pp. 2451 – 2464, Oct. 2002.

[6] P. Schniter, "Low-Complexity Equalization of OFDM in Doubly-Selective Channels," *IEEE Trans. Signal Processing*, vol. 52, pp. 1002–1011, Apr. 2004.

[7] Y. Zhao and S. Häggman, "Intercarrier Interference Self-Cancellation Scheme for OFDM Mobile Communication Systems," *IEEE Trans. Commun.*, vol. 49, pp. 1185 – 1191, July 2001.

[8] J. Armstrong, " Analysis of New and Existing Methods of Reducing Intercarrier Interference Due to Carrier Frequency Offset in OFDM," *IEEE Trans. Commun.*, vol. 47, pp. 365–369, Mar. 1999.

[9] H. Zhang and Y. Li, "Optimum Frequency-Domain Partial Response Encoding in OFDM," *IEEE Trans. Commun.*, vol. 51, pp. 1064–1068, July 2003.

[10] X. Ma, G. B. Giannakis, and S. Ohno, "Optimal Training for Block Transmissions over Doubly-Selective Fading Channels," *IEEE Trans. Signal Processing*, vol. 51, pp. 1351–1366, May 2003.

[11] S. Trautmann and N. J. Fliege, "A New Equalizer for Multitone Systems Without Guard Time," *IEEE Commun. Lett.*, vol. 6, pp. 34–36, Jan. 2002.

[12] S. Trautmann and N. J. Fliege, "Perfect Equalization for DMT Systems Without Guard Interval," *IEEE J. Select. Areas Commun.*, vol. 20, pp. 987–996, June 2002.

[13] N. Al-Dhahir and J. M. Cioffi, "Optimum Finite-Length Equalization for Multicarrier Transceivers," *IEEE Trans. Commun.*, vol. 44, pp. 56–64, Jan. 1996.

[14] K. van Acker, G. Leus, M. Moonen, O. van de Wiel, and T. Pollet, "Per-tone Equalization for DMT-based Systems," *IEEE Trans. Commun.*, vol. 49, Jan. 2001.

[15] I. Barhumi, G. Leus, and M. Moonen, "Frequency-Domain Equalization for OFDM over Doubly-Selective Channels," in *Sixth Baiona Workshop on Signal Processing in Communications*, (Baiona, Spain), pp. 103–107, Sept. 8-10 2003.

[16] I. Barhumi, G. Leus, and M. Moonen, "Time-Domain and Frequency-Domain Per-Tone Equalization for OFDM over Doubly-Selective Channels," *Signal Processing*, vol. 84/11, pp. 2055–2066, 2004. Special Section Signal Processing in Communications.

[17] I. Barhumi, G. Leus, and M. Moonen, "Time-Varying FIR Equalization of Doubly-Selective Channels," *IEEE Trans. Wireless Commun.*, Oct. 2003. (accepted).

[18] W. C. Jakes, ed., *Microwave Mobile Communications*. Wiley, 1974.

[19] G. B. Giannakis, Y. Hua, P. Stoica, and L. Tong, ed., *Signal Processing Advances in Wireless & Mobile Communications: Trends in Single and Multi-User Systems*. Prentice-Hall, Inc., 2001.

[20] G. B. Giannakis and C. Tepedelenlioğlu, "Basis Expansion Models and Diversity Techniques for Blind Identification and Equalization of Time-Varying Channels," *Proc. IEEE*, vol. 86, pp. 1969–1986, Oct. 1998.

[21] A. M. Sayeed and B. Aazhang, "Joint Multipath-Doppler Diversity in Mobile Wireless Communications," *IEEE Trans. Commun.*, vol. 47, pp. 123–132, Jan. 1999.

[22] X. Ma and G. B. Giannakis, "Maximum-Diversity Transmissions over Doubly-Selective Wireless Channels," *IEEE Trans. Inform. Theory*, vol. 49, pp. 1823–1840, July 2003.

[23] G. Leus, S. Zhou, and G. B. Giannakis, "Orthogonal Multiple Access over Time- and Frequency-Selective Fading," *IEEE Trans. Inform. Theory*, vol. 49, pp. 1942–1950, Aug. 2003.

[24] N. Al-Dhahir and J. Cioffi, "Efficiently Computed Reduced-Parameter Input-Aided MMSE Equalizers for ML Detection: A Unified Approach," *IEEE Trans. Inform. Theory*, vol. 42, pp. 903–915, May 1996.

[25] G. Ysebaert, K. Van Acker, M. Moonen, and B. De Moor, "Constraints in Channel Shortening Equalizer Design for DMT-based Systems," *Elsevier Signal Processing*, vol. 83, pp. 641–648, Mar. 2003.

[26] N. Al-Dhahir, "FIR Channel-Shortening Equalizers for MIMO ISI Channels," *IEEE Trans. Commun.*, vol. 49, pp. 213–218, Feb. 2001.

[27] B. Farhang-Boroujeny and S. Gazor, "Generalized Sliding FFT and its Application to Implementation of Block LMS Adaptive Filters," *IEEE Trans. Signal Processing*, vol. 42, pp. 532–538, Mar. 1994.

[28] G. Golub and C. V. Loan, *Matrix Computations*. Johns Hopkins University Press, third ed., 1996.

[29] Z. Wang and G. B. Giannakis, "Wireless Multicarrier Communications, where Fourier meets Shannon," *IEEE Signal Processing Mag.*, vol. 17, pp. 29–48, May 2000.

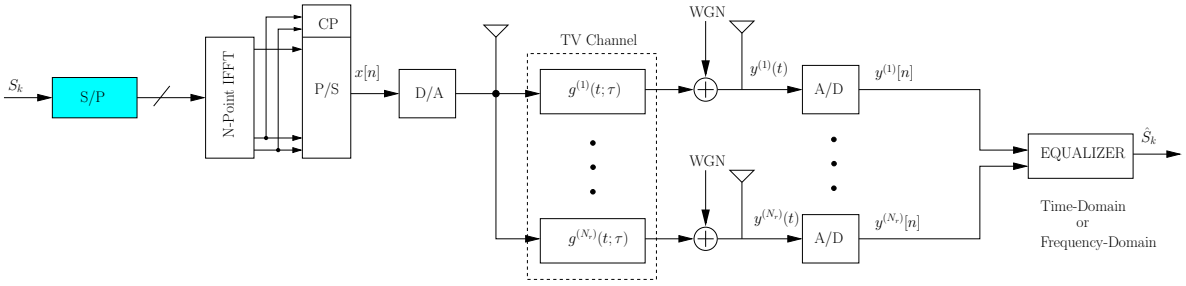


Fig. 1. System Model.

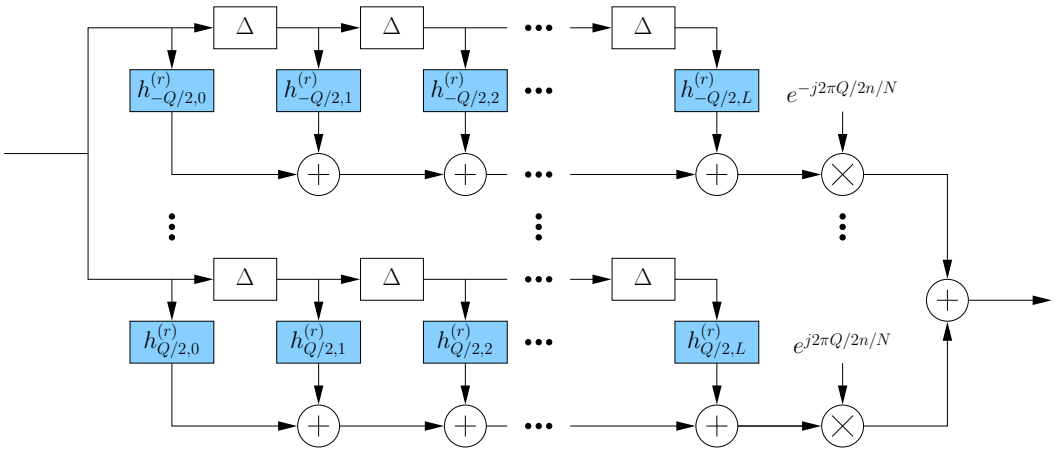


Fig. 2. BEM channel equivalent.

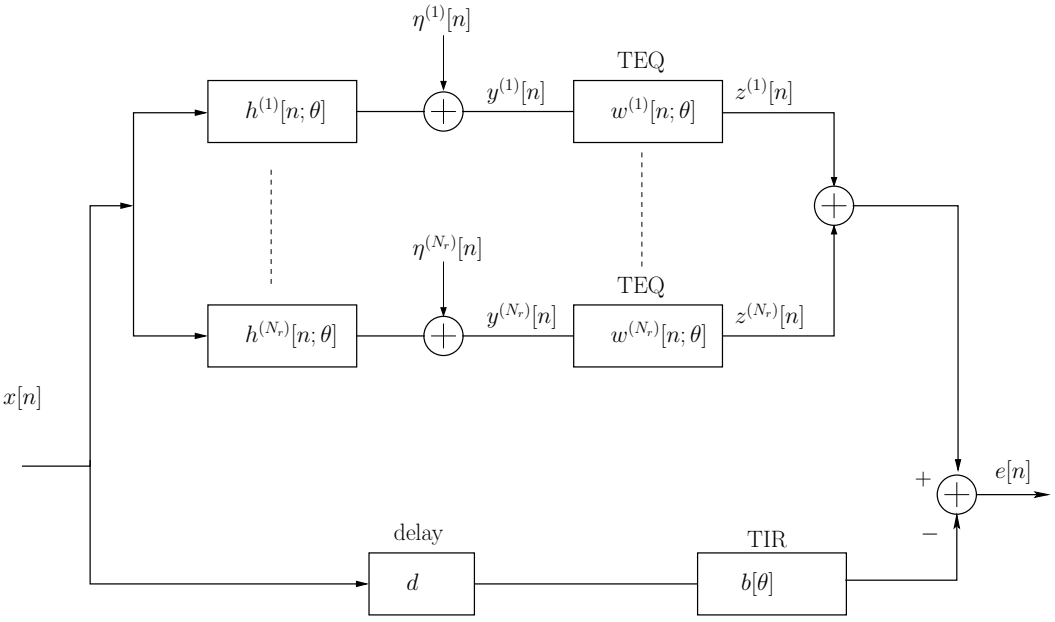


Fig. 3. TEQ equivalent figure.

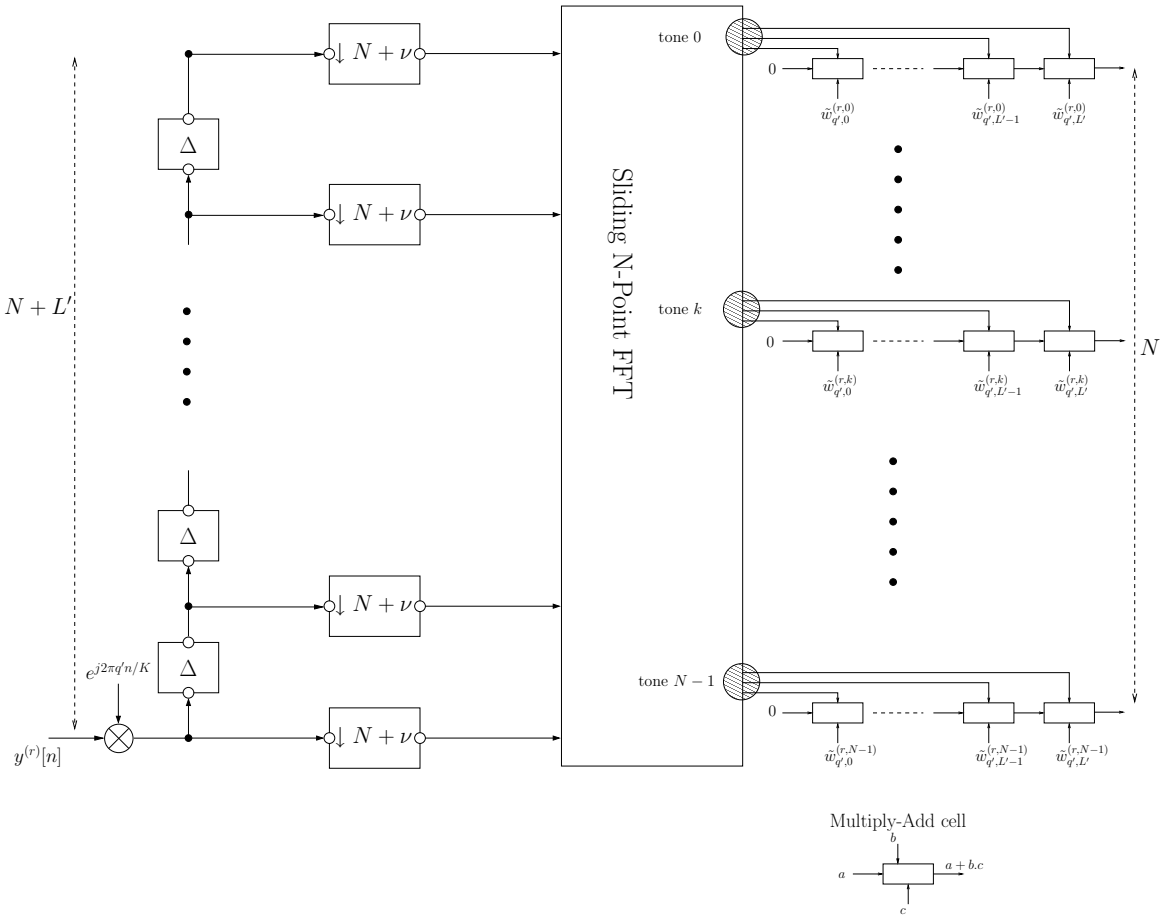


Fig. 4. Sliding FFT of the q'th modulated version of the received sequence $y^{(r)}[n]$.

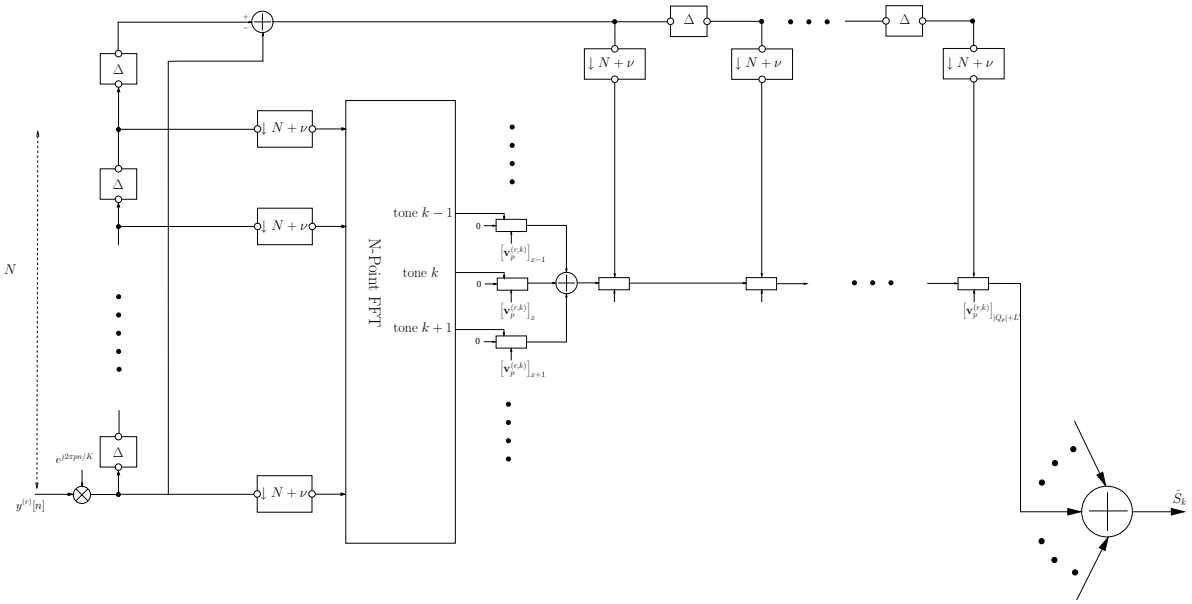


Fig. 5. Low complexity PTEQ.

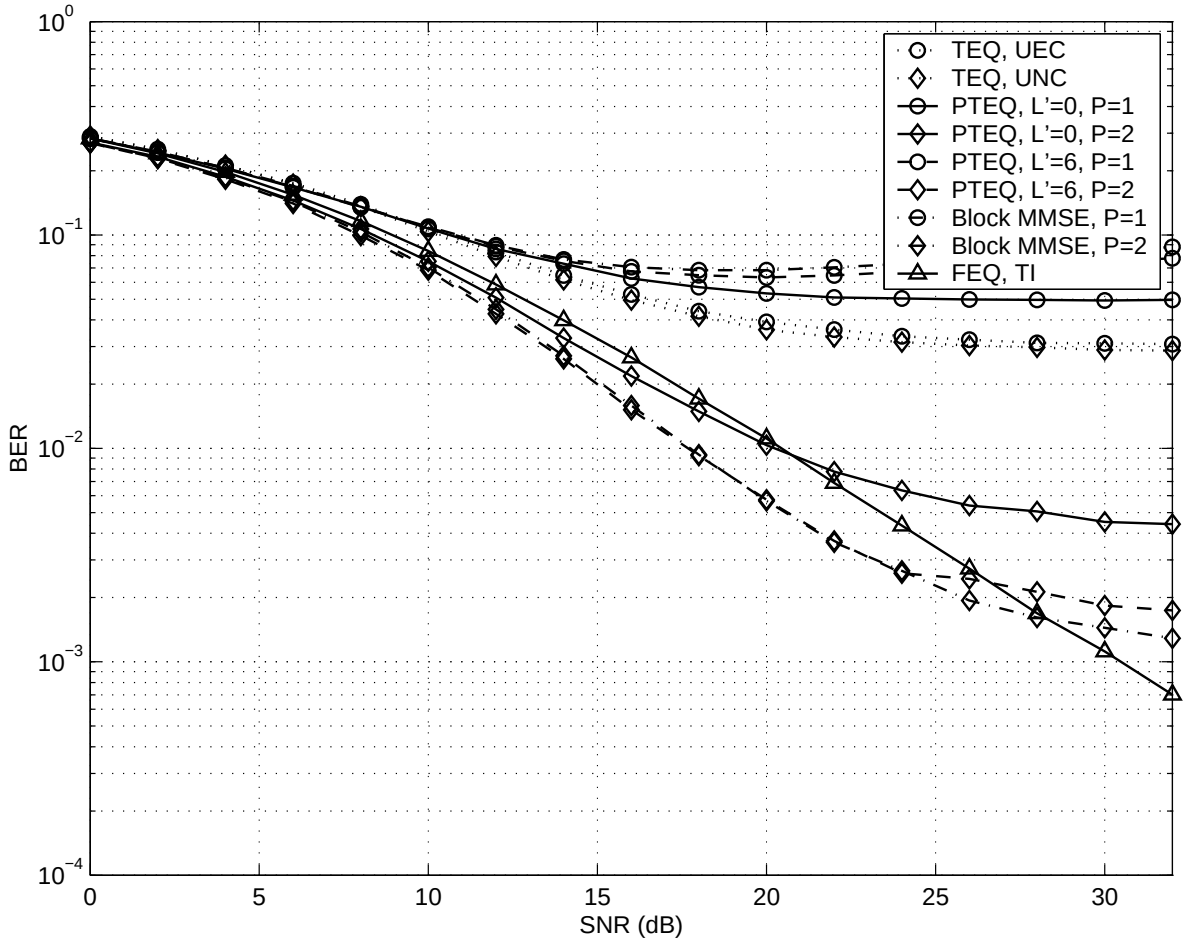


Fig. 6. BER vs. SNR for TEQ and PTEQ, $N_r = 1$ receive antenna.

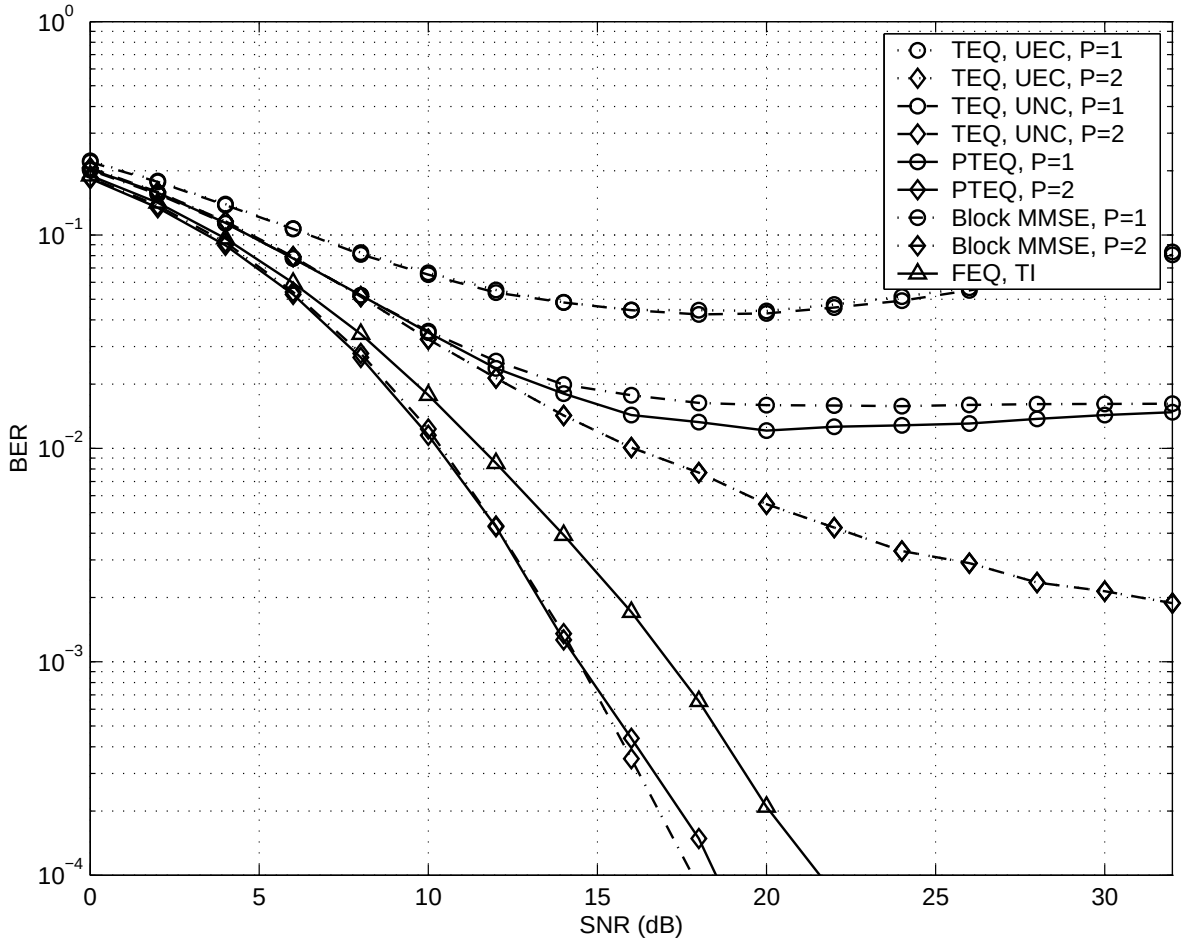


Fig. 7. BER vs. SNR for TEQ and PTEQ, $N_r = 2$ receive antennas.

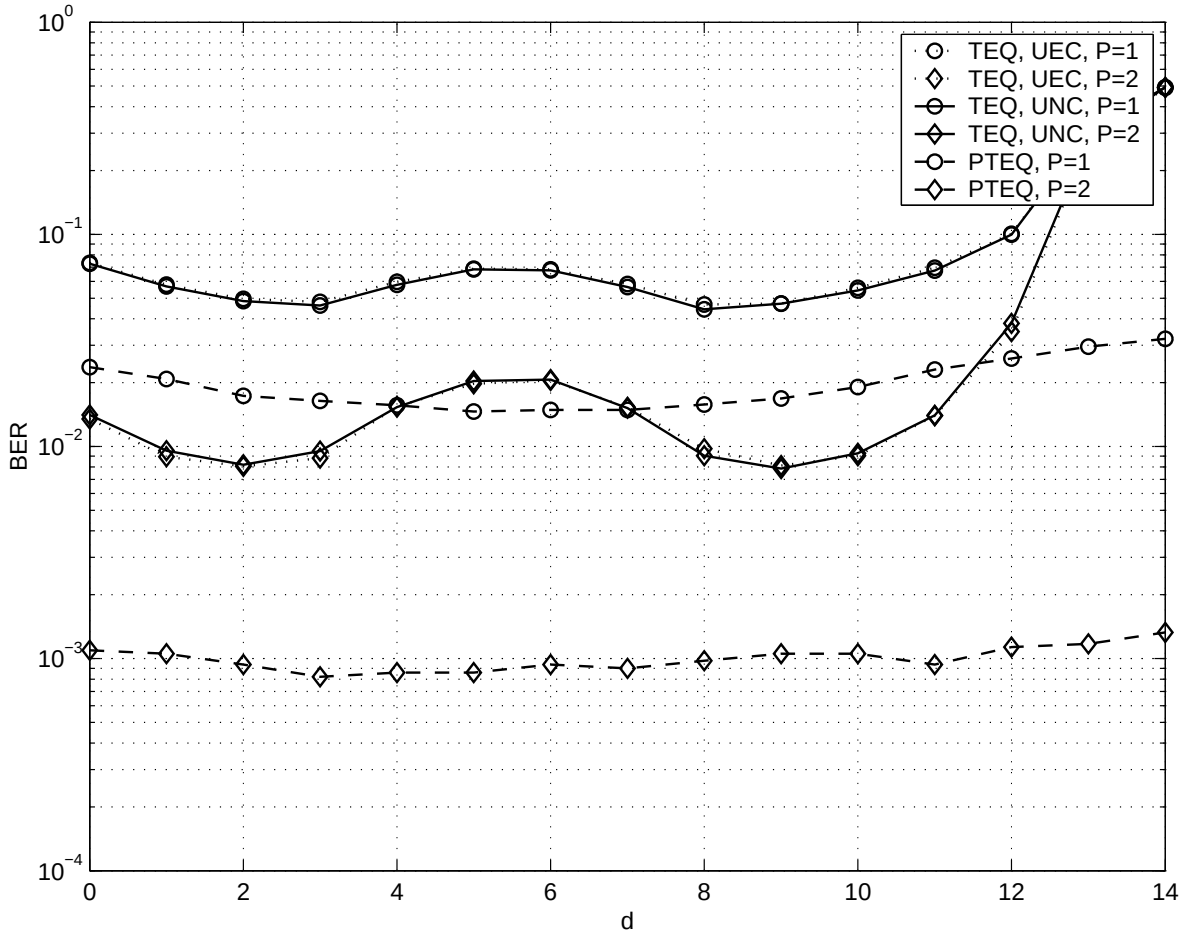


Fig. 8. BER vs. decision delay d for TEQ and PTEQ, $N_r = 2$ receive antennas at $SNR = 15\ dB$.

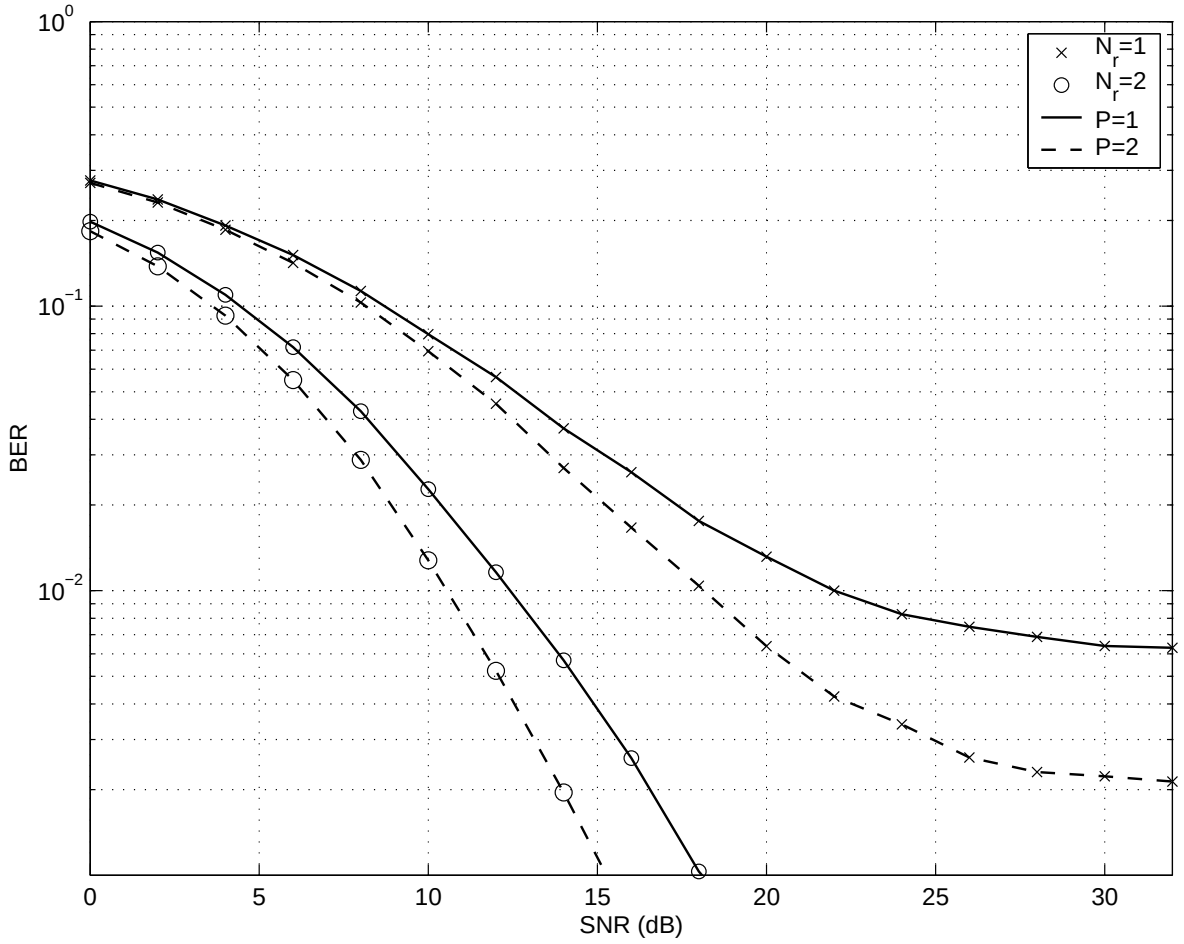


Fig. 9. BER vs. SNR for the PTEQ, when the true channel is used to design the equalizer.